GBT MEMO 209

Geometry And Conventions For Subreflector Metrology

M.A. Goldman

April 9, 2000

Abstract

This memo provides subreflector target location data and examines conceptual issues related to rangefinder metrology of the GBT subreflector surface. The following topics are addressed:

1. How does one use measured coordinates of subreflector range targets to describe spatial location and orientation of the subreflector surface? How should this information be made available to the subreflector servo control system, for the purpose of moving the subreflector to properly image from the prime focus defined by the main reflector surface to a secondary focus on the receiver room roof?

2. How does one aim feed arm and ground based rangefinders to hit subreflector range target prisms, given telescope elevation and azimuth encoder readouts, and displacement and tilt angle readouts of the subreflector encoders?

3. We define a geometric and linguistic format to discuss concepts and problems relating to rangefinder metrology of the subreflector. In particular, we define a telescope-coordinate-system-related subreflector home position and use a subreflector state vector to designate focus track command setting for the subreflector.

4. We compute and tabulate subreflector range target reference fiducial point coordinates and target prism axis direction components, with reference to both the subreflector and ellipsoid coordinate systems.

1. INTRODUCTION

1.1. Summary Of Telescope Geometry

1.1.1. Description Of A "Geometric GBT Telescope."

The physical embodiment of the GBT telescope focusing optics may be considered to be a geometrical configuration of two surfaces: a main reflector and a subreflector. As designed, the main reflector is a surface $\mathbf{P}$, (located somewhere in physical space) which is congruent to a surface patch $\mathbf{P}_s$, of a "Parent Paraboloid Of Revolution," $\mathbf{P}_{parent}$. The subreflector is a surface $\mathbf{E}$, (located somewhere in physical space) which is congruent to a surface patch $\mathbf{E}_s$, of a "Parent Ellipsoid Of Revolution," $\mathbf{E}_{parent}$. For the purposes of this memo, we will consider the subreflector and main reflector to be congruent, respectively, to surface patches of the parent ellipsoid and paraboloid.

The parent ellipsoid and parent paraboloid are mathematical constructs which are used to describe the ideal telescope design. The location of the parent ellipsoid is fixed relative to the parent paraboloid. The two *parent* surfaces are allowed to move together as a rigid bound pair in an abstract Euclidean 3-space R^3, equipped with a Cartesian coordinate system. The orientation of this pair of surfaces is described by two angle parameters: AZ_{com} and EL_{com}, commanded azimuth and elevation respectively.

The *as-built* surfaces $\mathbf{E}$ and $\mathbf{P}$, for the purposes of this memo, are each assumed to be a rigid surface patch of a quadric. But they are allowed to move independently of one another. When the subreflector $\mathbf{E}$, and main reflector $\mathbf{P}$, lie with respect to one another in the same configuration as the surface patches $\mathbf{E}_s$ and $\mathbf{P}_s$ of the parent surfaces lie for the ideal design telescope, the subreflector $\mathbf{E}$ will be said to "lie at home position" with respect to the main reflector $\mathbf{P}$. When the subreflector does not lie at home position, its location with respect to the main reflector will be described by means of three translation parameters

together with three rotation parameters, which we will describe subsequently.

There is some complexity associated with the definition and concept of a "home position" of the subreflector with respect to the main reflector. We discuss this below.

When the tipping structure of the as-built (physical) telescope is at or near to the telescope rigging elevation, the main reflector geometry will be close to that of the parent paraboloid, which has a 60 meter focal length. Near rigging elevation, the home position for the subreflector will be such that the symmetry planes of the subreflector and main reflector coincide, the F_0 (prime) focus point associated with the subreflector will lie at the focus of the main reflector paraboloid, and the line containing the two subreflector foci will make an angle $\beta = 5.570°$ with the paraboloid axis. An initial reference set of six subreflector actuator lengths will be measured during initial subreflector control system calibration, and will then define the control system state vector to bring the subreflector to its home position for rigging elevation. We note that the subreflector home position conceived in this manner will probably not be the subreflector position which will properly carry the telescope focus from prime focus (common to both reflector and subreflector) to the receiver room feed (the desired Gregorian focal point). To achieve proper focus, the receiver room must be aligned properly with respect to both the main reflector and subreflector surfaces at rigging elevation. However, a telescope with an initially misaligned receiver room at rigging elevation can be brought to focus by steering the subreflector. One changes the subreflector actuator lengths from their reference values for home position to values which best focus the telescope. We demand here that the subreflector home position will be defined for arbitrary telescope elevation, and will depend only on the relative positions of the primary and subreflector surfaces for each elevation, and will be independent of the position of the feed room and the mounting of the Stewart actuator platform.

When the telescope is driven to depart significantly from its rigging elevation, the main reflector's shape will be re-formed to a best fit paraboloid appropriate to the new elevation. The best fit paraboloid's focal length will depart from 60 meters, and the rotation of its axis will differ from the rotation of the elevation axle. The tilt of the Stewart platform supporting the subreflector, will change with respect to the telescope backup structure. The initial reference set of six actuator lengths will not then represent a subreflector position that has any telescope-

optical significance with respect to the main reflector. We wish, in principle, to define a home position for the subreflector at arbitrary telescope elevation. This home position should be defined to correspond to a geometric configuration of the telescope reflectors *which is optically meaningful.* Freedom of choice is available in making this definition.

The choice that we make is to define the subreflector home position (at any given commanded elevation) with reference to the *geometric telescope geometry* which corresponds to the design telescope configuration *at the commanded elevation angle*! Location of the subreflector is measured by prescribing its translational and rotational departures from the home position defined for the geometric telescope. We describe the general configuration of the subreflector by giving its position and orientation with respect to the main reflector reference frame of the design telescope, again at the given commanded elevation angle. The decision to reference the description of the physical telescope's configuration to the geometric design telescope configuration at commanded elevation angle is consistent with the subreflector control dynamics described in GBT Memo 183 [Wells-2].

An appendix: "The Reference Optical Telescope," originally in [Goldman-1], is included with this memo. It describes the geometry of the subreflector and its relation to that of the main reflector, for an ideal design telescope. The geometry of the geometric telescope's optics is illustrated in Figures 1 through 4.

1.1.2. Subreflector Motion Of The Geometric GBT Telescope.

The intrinsic geometry of the subreflector $\mathbf{E}$ is described by the "ellipsoid reference frame." This frame is characterized by three mutually perpendicular basis vectors: $\hat{X}_{ce}$, $\hat{Y}_{ce}$, $\hat{Z}_{ce}$ of unit length, and a frame origin point CE which is the center of the subreflector's ellipsoid. We attach to this frame a right-hand Cartesian coordinate system whose origin is at CE and whose coordinate axes lie in the directions of the frame basis vectors. The ellipsoid system coordinates of a point P are designated to be $X_{ce}(P)$, $Y_{ce}(P)$, $Z_{ce}(P)$. The reference ellipsoid is assumed to be embedded in real space so that its surface patch $\mathbf{P}_s$ coincides with the subreflector surface.

There exists a distinguished point embedded in the subreflector surface, the

subreflector reference point I_1. This point acts as an optical axis point for the ideal design telescope. That is, the *central ray* of the ray bundle leaving the prime focus of the ideal design telescope *passes through* I_1 and arrives at the Gregorian focus (which both lies at a feed horn flange center on the receiver room roof and also lies at a focus of the subreflector for the ideal telescope). The coordinates of this point are well defined. Referring to the design geometry illustrated in Figure 1, the coordinates of I_1 may be shown to be:

$$(1.1a) \qquad X_{ce}(I_1) \;=\; \frac{a}{\sqrt{1+(\frac{a}{b}\tan\alpha)^2}} \;=\; 9.736366 \text{ meters}$$

$$(1.1b) \qquad Y_{ce}(I_1) \;=\; X_{ce}(I_1)\cdot\tan\alpha \;=\; 3.144573 \text{ meters},$$

$$(1.1c) \qquad Z_{ce}(I_1) \;=\; 0.0 \text{ meters}.$$

It is necessary to also use another reference frame and coordinate system to describe position of the subreflector structure when it moves through ordinary 3-space. This is the "subreflector" reference frame. The subreflector frame is described by three mutually perpendicular unit length basis vectors: $\hat{X}_s$, $\hat{Y}_s$, $\hat{Z}_s$. The $(\hat{X}_s, \hat{Y}_s)$-plane is the plane of symmetry of the geometric telescope and the $\hat{Z}_s$ vector is perpendicular to this symmetry plane and directed towards the man-lift side of the telescope. The origin of the subreflector coordinate system is at the ideal (design) subreflector reference point I_1. The X_s, Y_s, Z_s coordinate axes point respectively along the $\hat{X}_s$, $\hat{Y}_s$, $\hat{Z}_s$ axes. That is:

$$(1.2) \qquad X_s(I_1) \;=\; 0\,, \quad Y_s(I_1) \;=\; 0\,, \quad Z_s(I_1) \;=\; 0\,.$$

The directions of the basis vectors $\hat{X}_s$, $\hat{Y}_s$ with respect to the ground reference frame of the telescope are well-defined functions of AZ_{com} and EL_{com} and are given explicitly later.

The subreflector frame is (together with its associated coordinate system) is used to describe motions of the subreflector when it is driven by its control system. Coordinate calculations tied to this reference frame are made by the telescope control system to generate Stewart platform actuator lengths, to position the subreflector. Computations referred to this frame are embedded in the telescope control system.

The subreflector frame orientation is tied nominally to that of the main reflector frame associated with the parent paraboloid and its surface patch $\mathbf{P}_s$, for a geometric telescope at the commanded elevation. The main reflector frame basis vectors $\hat{Y}_r$ and $\hat{Z}_r$ span a plane of symmetry of $\mathbf{P}_s$. The vector $\hat{Z}_r$ is directed along the axis of the parent paraboloid. The subreflector frame is oriented, by definition, so that the $(\hat{X}_s,\ \hat{Y}_s)$-plane is the same as the $(\hat{Y}_r,\ \hat{Z}_r)$-plane and the basis vector $\hat{Y}_s$ is rotated by precisely $36.7° \equiv \theta_s$ from $\hat{Z}_r$.

To describe subreflector drive motions D. Wells makes use of an additional drive axis, a "nutation axis," denoted by X_{nut}, which passes through the subreflector reference point and points in the direction of the unit vector $\hat{X}_{nut}$ which is defined in equations (1.3) below.

The unit vectors for the subreflector frame are expressed in terms of the unit basis vectors for the ellipsoid frame (Figure 7) by the relations:

$$
\begin{aligned}
\hat{X}_s &= S_{sce} \cdot \hat{X}_{ce} - C_{sce} \cdot \hat{Y}_{ce}\ , \\
\hat{Y}_s &= C_{sce} \cdot \hat{X}_{ce} + S_{sce} \cdot \hat{Y}_{ce}\ , \\
\hat{Z}_s &= \qquad \hat{Z}_{ce} \qquad\quad , \qquad\qquad \text{where}
\end{aligned}
\tag{1.3}
$$

$$
\begin{aligned}
S_{sce} &= \sin(\theta_s + \beta) = \sin(42.270°) = 0.6726251\,, \\
C_{sce} &= \cos(\theta_s + \beta) = \cos(42.270°) = 0.7399833\,, \qquad \text{and} \\
\hat{X}_{nut} &= C_s \cdot \hat{X}_s - S_s \cdot \hat{Y}_s\ , \quad \text{with} \quad C_s = \cos\theta_s \quad \text{and} \quad S_s = \sin\theta_s\ .
\end{aligned}
$$

The basis vectors for the subreflector frame are expressed in terms of the basis vectors for the main reflector frame by the relations:

$$
\begin{aligned}
\hat{X}_s &= \ C_s \cdot \hat{Y}_r + S_s \cdot \hat{Z}_r\ , \\
\hat{Y}_s &= -S_s \cdot \hat{Y}_r + C_s \cdot \hat{Z}_r\ , \\
\hat{Z}_s &= \qquad \hat{X}_r\ .
\end{aligned}
\tag{1.4}
$$

The subreflector's location relative to its home position is described by giving three angle deviations and three coordinate increments of displacement from home position. The subreflector home position corresponding to given telescope commanded elevation and azimuth is specified as follows: The main reflector reference frame is well-defined for the geometric telescope at arbitrary commanded elevation and azimuth. At home position, the subreflector parent ellipsoid is positioned so that the main reflector coordinates of the ellipsoid focus point F_0

are: $X_r(F_0) = 0$, $Y_r(F_0) = 0$, $Z_r(F_0) = 60$ meters; the ray F_1F_0 connecting the subreflector foci intersects the Z_r-axis at the angle $\beta = 5.570°$, and lies in the (Y_r, Z_r)-plane; the symmetry plane of the subreflector, which is the (X_{ce}, Y_{ce})-plane, coincides with the (Y_r, Z_r)-plane.

Displacements of the subreflector from its home position are specified by the position of its optical reference point. We use the symbol I_1 to denote the subreflector reference point at home position. We use the symbol I to denote the subreflector reference point when the subreflector is at a location other than at home position. Translation of the subreflector is then specified by the coordinates: $X_s(I)$, $Y_s(I)$, $Z_s(I)$. Rotations of the subreflector about the nutation axis X_{nut} and Y_s and Z_s axes are used to describe angular deviations of the subreflector from home position. The respective rotations of the subreflector are θ_{nut}, θ_y, θ_z, and are assumed to describe successive rotations about these axes, in the order given.

It is useful to describe the subreflector's general position by a "state vector" of the subreflector. We do this by defining the state vector to be list of eight quantities:

$$(1.5.1) \qquad \mathrm{S} = (AZ_{com}, EL_{com}, X_s(I), Y_s(I), Z_s(I), \theta_{nut}, \theta_y, \theta_z) \ .$$

In general, the state vector and its components are functions of time. In this memo, we will deal only with the geometry of the subreflector as a stationary object and ignore its explicit time variation.

The subreflector state vector corresponding to subreflector home position for arbitrary commanded angles of tipping structure elevation and azimuth is:

$$(1.5.2) \qquad \mathrm{S}_{\mathrm{hp}}(AZ_{com}, EL_{com}) = (AZ_{com}, EL_{com}, 0, 0, 0, 0, 0, 0).$$

The subreflector reference frame unit basis vectors corresponding to the configuration of the geometric design telescope oriented at azimuth AZ_{com} and elevation EL_{com} are defined to be:

$$(1.5.3)\qquad \begin{bmatrix} \hat{X}_s \\ \hat{Y}_s \\ \hat{Z}_s \end{bmatrix} = \begin{bmatrix} -S_{sE}\cdot\sin AZ_{com} & -S_{sE}\cdot\cos AZ_{com} & -C_{sE} \\ -C_{sE}\cdot\sin AZ_{com} & -C_{sE}\cdot\cos AZ_{com} & S_{sE} \\ -\cos AZ_{com} & \sin AZ_{com} & 0 \end{bmatrix} \cdot \begin{bmatrix} \hat{X} \\ \hat{Y} \\ \hat{Z} \end{bmatrix}$$

in terms of the ground frame basis vectors, and where

$$(1.5.4)\qquad S_{sE} = \sin(EL_{com} + \theta_s)\ , \quad C_{sE} = \cos(EL_{com} + \theta_s) \quad \text{where } \theta_s \equiv 36.7^\circ.$$

The basis vectors defined by (1.5.3) are also considered to be the subreflector frame basis vectors, and the subreflector frame origin point is considered to be at the reference point I_1 independent of the values of θ_{nut}, θ_y, θ_z for the above-commanded azimuth and elevation angles. That is we require by definition, that the subreflector reference frame and coordinate system depend only on the commanded orientation of the telescope's main reflector surface and do not depend on the subreflector's commanded tilt angles.

1.1.3. Subreflector Reference Points.

The mounting geometry for the rangefinder retroreflector targets on the subreflector is illustrated in Figure 6. A cube corner prism target, j, is referenced by its fiducial point, T_j, having coordinates $X_{ce}(T_j)$, $Y_{ce}(T_j)$, $Z_{ce}(T_j)$ in the parent ellipsoid coordinate system. These coordinates are constants which are independent of the telescope motions, to the extent that the subreflector surface is rigid. We assume this to be the case. A target is also characterized by its corner vertex point and its pedal point PP_j which is the foot of the perpendicular from the vertex point to the opposite prism face, the ray entry face. The prism axis is the line passing through both the vertex and pedal points. Reference point T_j lies on the prism axis, at a distance $\dfrac{D_j}{n}$ from PP_j, where D_j is the prism depth and $n \simeq 1.527077$ is the ratio of the group speed of light of BK7 prism glass to that of air. Point T_j is the effective range target point for rangefinder metrology. We give the name $\hat{N}_j$ to the unit vector along the direction of the prism axis of target j, in the sense directed from PP_j into the subreflector interior. We name the direction cosines of $\hat{N}_j$ with respect to the X_{ce}, Y_{ce}, Z_{ce}-axes respectively: N_{xce}, N_{yce}, N_{zce}.

There is a unique surface point of the subreflector ellipsoid associated with each target fiducial point. We call Q_j the unique point on the subreflector surface which is associated with target j. Point Q_j is the intersection point of the prism axis with the subreflector surface. We give the name $\hat{n}(Q_j)$ to the unit vector normal to the ellipsoid surface at Q_j, in the sense directed from Q_j into the subreflector interior. We name the direction cosines of $\hat{n}_j$ with respect to the X_{ce}, Y_{ce}, Z_{ce}-axes respectively: n_{xce}, n_{yce}, n_{zce}.

In general, points PP_j and Q_j could be distinct, with a distance D_{poj} between them. However the targets have been designed and mounted into the subreflector structure so that the prism pedal point coincides with the subreflector surface point, so that $PP_j = Q_j$, and $D_{poj} = 0$.

The prism axes have been rotated from the surface normals to improve viewing by feed arm rangefinders. Care was taken to mount the targets so that the axis of target j lies in the plane generated by point Q_j and the X_{ce}-axis. The surface normal Q_j, the ellipsoid major X_{ce}-axis, and the prism axis are all co-planar. The direction of $\hat{N}_j$ is rotated from that of $\hat{n}(Q_j)$ by an angle Ψ_j, which was selected to give good target visibility from the feed arm rangefinders. Prism offset angles and depths are given in Table 2. A copy of the prism mount construction drawing [Taggart-1] is included with this memo.

The Unit Surface Normal Vector At A Subreflector Surface Point.

The direction cosines of the unit normal vector to the subreflector ellipsoid at a surface point Q_j are computed as follows. From the equation of the ellipsoid,

$$\frac{X_{ce}^2}{a^2} + \frac{Y_{ce}^2 + Z_{ce}^2}{b^2} - 1 = 0 \quad , \tag{1.6.1}$$

one can derive the equation of the tangent plane at Q_j:

$$\frac{X_{ce} \cdot X_{ce}(Q_j)}{a^2} + \frac{Y_{ce} \cdot Y_{ce}(Q_j)}{b^2} + \frac{Z_{ce} \cdot Z_{ce}(Q_j)}{b^2} - 1 = 0 \quad , \tag{1.6.2}$$

which can also be written in terms of the direction cosines of the unit surface normal vector at Q_j, with respect to the ellipsoid frame coordinate axes, as:

$$X_{ce} \cdot n_{xce}(Q_j) + Y_{ce} \cdot n_{yce}(Q_j) + Z_{ce} \cdot n_{zce}(Q_j) - 1 = 0 \quad . \tag{1.6.3}$$

Comparing terms, and using the fact that the sum of the squares of the direction cosines is one, and choosing the sign appropriately so that the vector points towards the ellipsoid's interior one gets:

$$n_{xce}(Q_j) = \frac{-X_{ce}(Q_j)}{\sqrt{X^2_{ce}(Q_j) + (\frac{a^4}{b^4})(Y^2_{ce}(Q_j) + Z^2_{ce}(Q_j))}} \quad , \tag{1.6.4a}$$

$$n_{yce}(Q_j) = \frac{-Y_{ce}(Q_j)}{\sqrt{(\frac{b^4}{a^4}) \cdot X^2_{ce}(Q_j) + (Y^2_{ce}(Q_j) + Z^2_{ce}(Q_j))}} \quad , \tag{1.6.4b}$$

$$n_{zce}(Q_j) = \frac{-Z_{ce}(Q_j)}{\sqrt{(\frac{b^4}{a^4}) \cdot X^2_{ce}(Q_j) + (Y^2_{ce}(Q_j) + Z^2_{ce}(Q_j))}} \quad . \tag{1.6.4c}$$

The Unit Vector Along The Axis Of A Target Prism.

Here we calculate (in the ellipsoid coordinate system) the direction cosines of a unit vector $\hat{N}_j$ pointing outwards from the pedal point of subreflector target prism j along the direction of the prism axis. The relevant geometry is shown in Figure 6. We start from the defining relations in terms of direction cosines,

$$\hat{N}_j \equiv N_{xce} \cdot \hat{X}_{ce} + N_{yce} \cdot \hat{Y}_{ce} + N_{zce} \cdot \hat{Z}_{ce} \quad , \tag{1.7.1}$$

$$\hat{n}(Q_j) \equiv n_{xce} \cdot \hat{X}_{ce} + n_{yce} \cdot \hat{Y}_{ce} + n_{zce} \cdot \hat{Z}_{ce} \quad . \tag{1.7.2}$$

The surface normal vector and the prism axis unit vector at Q_j both lie in the plane defined by point Q_j and the X_{ce}-axis, which is the ellipsoid major axis. In that plane $\hat{N}_j$ lies at Ψ_j angle to $\hat{n}(Q_j)$. We note that the vector

$$\hat{u}_j \equiv \frac{\hat{X}_{ce} \times \hat{n}(Q_j)}{\left|\hat{X}_{ce} \times \hat{n}(Q_j)\right|} \tag{1.7.3}$$

is a unit vector which is $\perp$ to the plane of Q_j and the X_{ce}-axis. Thus

$$\hat{n}(Q_j) \cdot \hat{u}_j = 0 \qquad \text{and} \qquad \hat{N}_j \cdot \hat{u}_j = 0 \, . \tag{1.7.4}$$

We express $\hat{u}_j$ in terms of ellipsoid frame basis vectors.

$$(1.7.6) \qquad \hat{u}_j \;=\; u_{xj}\cdot\hat{X}_{ce} + u_{yj}\cdot\hat{Y}_{ce} + u_{zj}\cdot\hat{Z}_{ce}\;.$$

Computing $\hat{u}_j$ explicitly from (1.7.3), one gets

$$(1.7.7) \quad u_{xj} \;=\; 0\;, \quad u_{yj} \;=\; \frac{-n_{zce}}{\sqrt{n_{yce}^2 + n_{zce}^2}}\;, \quad u_{zj} \;=\; \frac{n_{yce}}{\sqrt{n_{yce}^2 + n_{zce}^2}}\;.$$

We generate $\hat{N}_j$ by rotating $\hat{n}(Q_j)$ about an axis along $\hat{u}_j$ by a right-hand angle, Ψ_j. Using $\hat{n}(Q_j)\cdot\hat{u}_j = 0$ we get

$$(1.7.8) \qquad \hat{N}_j \;=\; (\cos\Psi j)\cdot\hat{n}(Q_j) + (\sin\Psi j)\cdot(\hat{n}(Q_j)\times\hat{u}_j)\;.$$

Using the abbreviations

$$(1.7.9) \qquad C_\Psi \;\equiv\; \cos\Psi_j \quad\text{and}\quad S_\Psi \;\equiv\; \sin\Psi_j$$

and the identity $n_{xce}^2 + n_{yce}^2 + n_{zce}^2 \equiv 1$, we get, after manipulation of (1.6.7) and (1.6.8):

$$(1.7.10) \qquad \begin{aligned} N_{xce} &= (C_\Psi\cdot n_{xce}) + (S_\Psi\cdot\sqrt{1-n_{xce}^2})\;,\\ N_{yce} &= \left(C_\Psi\cdot n_{yce} - \frac{S_\Psi\cdot n_{xce}\cdot n_{yce}}{\sqrt{1-n_{xce}^2}}\right)\;,\\ N_{zce} &= \left(C_\Psi\cdot n_{zce} - \frac{S_\Psi\cdot n_{xce}\cdot n_{zce}}{\sqrt{1-n_{xce}^2}}\right)\;. \end{aligned}$$

Numerical values are given in Table 2.

1.2. Symbols

Definitions of symbols used in this memo are given in Table 1.

Table 1: List Of Symbols.

Symbol	Meaning
T_j	Fiducial reference point of target j.
$X(T_j)$	Ground coordinate of target j.
$Y(T_j)$	Ditto.
$Z(T_j)$	Ditto.
a, b	Parent ellipsoid semi-axes (a>b).
F_0, F_1	Foci of parent ellipsoid.
I_1	Reference point of parent ellipsoid.
V_p	Vertex point of parent paraboloid.
F_p	Focal point of parent paraboloid.
$\beta \equiv 5.570$	$\angle F_1F_0V_p$ for design telescope.
$\alpha \equiv 17.899°$	$\angle F_0F_1I_1$ for design telescope.
$\gamma = 36.127028°$	$\angle F_0I_1F_1$ for design telescope.
$\theta_s \equiv 36.7°$	Tilt of subreflector frame to main reflector frame.
CE	Center point of parent ellipsoid.
I	Image of I_1 under subreflector translation.
$X_s(I)$	Translation components of the
$Y_s(I)$	subreflector reference point
$Z_s(I)$	from home position.
X_{nut}	Nutation axis (in subreflector frame).
$\theta_x \equiv \theta_{nut}$	Subreflector tilt about nutation axis.
θ_y	Subreflector tilt about the Y_s-axis.
θ_z	Subreflector tilt about the Z_s-axis.
AZ_{com}	Commanded telescope azimuth.
EL_{com}	Commanded telescope elevation.

Symbol	Meaning
$X_{ce}(T_j)$	Ellipsoid frame coordinates
$Y_{ce}(T_j)$	of fiducial reference point
$Z_{ce}(T_j)$	of the prism retrotarget j.
$X_s(T_j)$	Subreflector frame coordinates
$Y_s(T_j)$	of fiducial reference point
$Z_s(T_j)$	of the prism retrotarget j.
$N_{xce}(j)$	Direction cosines of normal
$N_{yce}(j)$	to prism entry face
$N_{tce}(j)$	for retrotarget j.
Ψ_j	Offset angle of prism axis to surface normal.
C_s, S_s	$C_s = \cos\theta_s,\ S_s = \sin\theta_s,\ \theta_s \equiv 36.7°$
C_β, S_β	$C_\beta = \cos\beta,\ S_s = \sin\beta,\ \beta \equiv 5.570°$
C_{sce}, S_{sce}	$C_{sce} = \cos(\theta_s + \beta),\ S_{sce} = \sin(\theta_s + \beta)$
C_{sE}, S_{sE}	$C_{sE} = \cos(EL_{com} + \theta_s),\ S_{sE} = \sin(EL_{com} + \theta_s)$
$\vec{v}$	Arrow denotes a vector.
$\widehat{u}$	Carat denotes a unit length vector.
Q_j	Surface point associated with target j.
$\hat{n}_j$	Unit normal to ellipsoid surface at Q_j.
D_j	Depth of prism retrotarget j.
PP_j	Pedal point of retrotarget j.
$\hat{N}_j$	Unit normal to prism face at PP.
δ_{xj}	$X_{ce}(T_j) - X_{ce}(I_1)$
δ_{yj}	$Y_{ce}(T_j) - Y_{ce}(I_1)$
δ_{zj}	$Z_{ce}(T_j) - Z_{ce}(I_1)$
$\mathbf{S}$	Subreflector state vector.

Symbol	Meaning
$X_{xsj}(\mathbf{S})$	Subreflector system coordinates
$Y_{ysj}(\mathbf{S})$	for retrotarget reference point T_j,
$Z_{zsj}(\mathbf{S})$	with subreflector at state vector $\mathbf{S}$.
$N_{xsj}(\mathbf{S})$	Prism axis direction cosines to
$N_{ysj}(\mathbf{S})$	subreflector coordinate system
$N_{zsj}(\mathbf{S})$	axes, subreflector at state vector $\mathbf{S}$.
A	Integer used to index target triples.
$T_1(A)$, $T_2(A)$, $T_3(A)$	Triple of subreflector retrotargets.
$F(A), G(A), H(A)$	Barycentric target coordinates.
	for subreflector reference point I
	for a given retrotarget triple.
N^{hp}_{xsj}	Prism axis direction cosines to
N^{hp}_{ysj}	subreflector coordinate system
N^{hp}_{zsj}	axes, subreflector at home position.
$X_{shp}(T_j)$	Subreflector system coordinates of
$X_{shp}(T_j)$	retrotarget reference point T_j,
$X_{shp}(T_j)$	for subreflector at home position.
$f_{xs}(A)$, $g_{xs}(A)$, $h_{xs}(A)$	Barycentric coordinates of $\hat{X}_s$,
$f_{ys}(A)$, $g_{ys}(A)$, $h_{ys}(A)$	barycentric coordinates of $\hat{Y}_s$,
$f_{zs}(A)$, $g_{zs}(A)$, $h_{zs}(A)$	barycentric coordinates of $\hat{Z}_s$,
	for a given retrotarget triple.
$\hat{t}_{12}(A)$	Unit vector directed from $T_1(A)$ to $T_2(A)$.
$\hat{t}_{13}(A)$	Unit vector directed from $T_1(A)$ to $T_3(A)$.
$\hat{t}_{cp}(A)$	Unit vector $\perp$ to $\hat{t}_{12}(A)$ and $\hat{t}_{13}(A)$.

1.3. Subreflector Prism Target Description

Computed values for the parameters describing the subreflector range prism targets, as mounted, are given in Table 2.

Table 2: Subreflector Prism Target Parameters (As-built).

(j)	Subreflector		Ψ_j	$X_{ce}(T_j)$ (m)	$Y_{ce}(T_j)$ (m)	$Z_{ce}(T_j)$ (m)
	Target			$N_{xce}(Q_j)$	$N_{yce}(Q_j)$	$N_{zce}(Q_j)$
ZSG305	Uppermost	(#1)	03.8°	10.372578	0.912271	0.103002
				−0.982329	−0.185979	−0.020998
ZSG312	Upper Left	(#3)	20.1°	9.335102	2.609955	−2.962032
				−0.636790	−0.509739	0.578502
ZSG313	Upper Right	(#8)	20.1°	9.332404	2.614406	2.964014
				−0.636315	−0.510296	−0.578534
ZSG316	Lower Left	(#9)	32.1°	7.323294	5.276288	−3.450458
				−0.137510	−0.828977	0.542114
ZSG317	Lower Right	(#6)	32.1°	7.325431	5.271887	3.454404
				−0.137770	−0.828455	−0.542845
ZSG321	Lowermost	(#5)	37.2°	5.923326	7.287701	0.083961
				0.117971	−0.992951	−0.011440

Coordinates in Table 2 are those of the retroprism target fiducial reference points as mounted, calculated from photogrammetrically measured surface point coordinates given in Table 3, and measured prism depth and mounting offset angle Ψ_j. The direction cosines of each prism's axis are computed using the prism offset angle and direction cosines of the associated surface point's normal vector given in Table 3.

Target reference point coordinates were computed using a measured prism depth $D = 0.7403$ inches for each of the six subreflector targets. The target range correction constant corresponding to this prism depth is: $P_c = -D(n - \frac{1}{n}) = -0.6457$ inches $= -0.016401$ meters.

Computed values of distance between subreflector reference points are given below.

Table 2b: Computed Distances Between Subreflector Reference Points

Fiducial Reference Point P1	Fiducial Reference Point P2	Distance D(P1, P2) (meters)
I_1	ZSG305	2.3234777
I_1	ZSG312	3.0365219
I_1	ZSG313	3.0380324
I_1	ZSG316	4.7194051
I_1	ZSG317	4.719214
I_1	ZSG321	5.6313256
ZSG305	ZSG312	3.6541647
ZSG305	ZSG313	3.4877816
ZSG305	ZSG316	6.4007697
ZSG305	ZSG317	6.2867527
ZSG305	ZSG321	7.7744653
ZSG312	ZSG313	5.9260486
ZSG312	ZSG316	3.3756872
ZSG312	ZSG317	7.2315503
ZSG312	ZSG321	6.5421402
ZSG313	ZSG316	7.2296325
ZSG313	ZSG317	3.3660996
ZSG313	ZSG321	6.4619034
ZSG316	ZSG317	6.9048640
ZSG316	ZSG321	4.3009080
ZSG317	ZSG321	4.1700467

Distances in Table 2b are calculated from the ellipsoid frame coordinates $X_{ce}(T_j), Y_{ce}(T_j), Z_{ce}(T_j)$, of the retroprism target fiducial reference points as mounted, calculated from photogrammetrically measured surface point coordinates given in Table 3, and measured prism depth and mounting offset angle Ψ_j. The coordinates assumed for the subreflector reference point I_1 are theoretical values calculated from the design equations (1.1).

Table 3: Measured Subreflector Surface Point Coordinates (meters), and Surface Point Normal Vector Direction Cosines.

(j)	Subreflector	$X_{ce}(Q_j)$	$Y_{ce}(Q_j)$	$Z_{ce}(Q_j)$
	Target	$n_{xce}(Q_j)$	$n_{yce}(Q_j)$	$n_{yce}(Q_j)$
ZSG305	Uppermost	10.360482	0.909980	0.102743
		-0.992574	-0.120879	-0.013648
ZSG312	Upper Left	9.327261	2.603678	-2.954909
		-0.862980	-0.334017	0.379075
ZSG313	Upper Right	9.324569	2.608123	2.956890
		-0.862669	-0.334563	-0.379302
ZSG316	Lower Left	7.321601	5.266080	-3.443783
		-0.642838	-0.641088	0.419243
ZSG317	Lower Right	7.323734	5.261686	3.447720
		-0.643039	-0.640567	-0.419732
ZSG321	Lowermost	5.924779	7.275474	0.083820
		-0.506410	-0.862236	-0.009934

Coordinates given in Table 3 are for measured centers of photogrammetry targets at the subreflector surface, set to lie at the pedal points of prism retroreflector targets to be inserted at the respective target locations. They are taken from F. Schwab's, unpublished note: "Corrected version of table," Feb. 26, 1999. Coordinates given in that note have been converted to meters.

Table 4: Target Fiducial Reference Point (Subreflector System) Coordinates When Subreflector Is At Home Position.

(j)	Subreflector	$X_{shp}(T_j)$	$Y_{shp}(T_j)$	$Z_{shp}(T_j)$
	Target	meters	meters	meters
ZSG305	Uppermost	2.0797988	-1.0307164	0.1030016
ZSG312	Upper Left	0.1257086	-0.6565264	-2.9620324
ZSG313	Upper Right	0.1205994	-0.6555287	2.9640140
ZSG316	Lower Left	-3.2005263	-0.351788	-3.4504581
ZSG317	Lower Right	-3.1958326	-0.3531667	3.4544041
ZSG321	Lowermost	-5.6305920	-0.03531667	0.0839609

1.4. Subreflector Location From Range Target Coordinates

Here, we present computations which give the coordinates of the subreflector reference point I, and the directions of the subreflector axes when the subreflector is no longer at home position. We assume that we possess measured values for coordinates of some of the subreflector retrotarget fiducial points. (These coordinates are assumed to have been obtained by laser ranging from either feed arm or ground rangefinders, and subsequent reduction and adjustment of the range measurements). The problem which we solve is to locate the subreflector, starting from adjusted coordinates of some of its reference target points.

We start with measured and adjusted coordinates of at least three subreflector retrotarget reference points. These are allowed to be either ground frame coordinates or main reflector coordinates. These coordinates are converted to the subreflector reference frame using the standard GBT coordinate transformations. We will then compute the subreflector frame coordinates of the subreflector reference point I, and the orientations of the subreflector ellipsoid's axes. The computed displacement components $X_s(I)$, $Y_s(I)$, $Z_s(I)$ are three of the six local subreflector coordinates used to describe the subreflector displacement from its home position (consistent with commanded main reflector azimuth AZ_{com} and elevation EL_{com}). The subreflector tilt angles θ_{nut}, θ_y, θ_z can then be computed subsequently from the tilt of the ellipsoid axes. We will not carry out that involved computation in this memo; we will here obtain the rotated ellipsoid axes and leave the final computations of the tilt angles to a later document. The information generated in this section will locate the subreflector in space. It can be used later to provide the subreflector motion drive system with observed subreflector frame state vector components, which correspond to the actual actuator drive setpoints existing when the subreflector is at the measured position.

Following these calculations (in Section 1.4) we will subsequently solve the inverse problem (in Section 1.5); we will compute coordinates for subreflector retrotarget reference points and their prism axis directions for a general commanded position of the subreflector. The latter computations will provide target reference point coordinates and target prism axis direction cosines needed for rangefinder aiming and target visibility calculations.

1.4.1. Determination Of Subreflector Reference Point Position

The metrology problem to be addressed in this section is the following. We assume that we know adjusted coordinates of three or more subreflector retrotarget fiducial points with respect to ground reference frame coordinate system. These are obtained by range measurements to three or more subreflector retrotargets. The measurements have been least-squares-adjusted. We are also given a set of commanded values for the six subreflector state variables, together with commanded values for telescope elevation and azimuth, which were set to drive the subreflector to the position where it was measured. By calculating (from the adjusted measurement coordinates of the retrotarget reference points) the location of the origin and the orientation of the subreflector reference frame (corresponding to the given commanded telescope azimuth and elevation), we can compute the actual existing displacement of the subreflector reference point from the subreflector frame origin and the tilt angles of the subreflector. We can then compare the values of $X_s(I)$, $Y_s(I)$, $Z_s(I)$, θ_{nut} , θ_y , θ_z derived from rangefinder measurements to the setpoint values for these quantities, which were commanded by the subreflector drive control system.

It is possible to compute a least-squares fit of the subreflector position using the adjusted subreflector target fiducial point locations for all of the measured targets. This has been recommended (private conversation) by D. Wells. If one does this, one should keep in mind (in setting up this least-squares procedure) that the adjusted range measurements give coordinates of target fiducial reference points and not ellipsoid surface points. We will now present a procedure which will generate the subreflector frame coordinates of reference point I from adjusted measurement coordinates of the fiducial reference points of three arbitrary subreflector retrotargets. There are $\binom{6}{3} = 20$ combinations of three targets whose reference point coordinates can be used to find subreflector position. We will give linear relations for the subreflector system position coordinates of the subreflector reference point I, together with the direction cosines of the rotated subreflector basis vectors $\mathcal{R}[\hat{X}_s]$, $\mathcal{R}[\hat{Y}_s]$, $\mathcal{R}[\hat{Z}_s]$ with respect to the ground frame coordinate system.

We start with the following assumptions:

- Ground frame coordinates of at least three subreflector prism retrotargets were measured by rangefinders (and the range measurements were reduced

and least-squares adjusted). These are the coordinates of the fiducial reference points of the subreflector target prisms. The subreflector need not have been at home position when the measurements were made.

- We also assume that commanded setpoint values for the three subreflector offset angles and three subreflector reference point displacement coordinates for the time of measurement are known.

The measurement situation is static. That is, the telescope is not moving.

We assume that the three subreflector targets have adjusted coordinates: X_1, Y_1, Z_1; X_2, Y_2, Z_2; X_3, Y_3, Z_3 respectively, with respect to some right-hand rectangular Cartesian coordinate system, whose orthogonal unit basis vectors we call $\hat{X}, \hat{Y}, \hat{Z}$. We will not specify *which* system, at the present moment. We will call the displacement vectors of these three targets and of the subreflector reference point I, with respect to the origin of this coordinate system

$$
\begin{aligned}
\vec{I} &= X(I)\cdot\hat{X} + Y(I)\cdot\hat{Y} + Z(I)\cdot\hat{Z}\,, \\
\vec{T_1} &= X_1\cdot\hat{X} + Y_1\cdot\hat{Y} + Z_1\cdot\hat{Z}\,, \\
\vec{T_2} &= X_2\cdot\hat{X} + Y_2\cdot\hat{Y} + Z_2\cdot\hat{Z}\,, \\
\vec{T_3} &= X_3\cdot\hat{X} + Y_3\cdot\hat{Y} + Z_3\cdot\hat{Z}\,.
\end{aligned}
\tag{1.4.1}
$$

We can use barycentric coordinates to describe the location of a reference point embedded in the subreflector. Those coordinates will be constants which are independent of the particular reference frame and basis vectors used to give point coordinates. For each triple: T_1, T_2, T_3 of measured target reference points we can find three scalar constants: $F(T_1, T_2, T_3)$, $G(T_1, T_2, T_3)$, $H(T_1, T_2, T_3)$ which give the coordinates of I in terms of the coordinates of these target points. The coordinates of I appear in the same coordinate system for which the coordinates of the target points are given! The procedure for doing this is the following. We write,

$$
\vec{I} = \left(\frac{1}{3}\right)(\vec{T_1}+\vec{T_2}+\vec{T_3}) + F\cdot(\vec{T_2}-\vec{T_1}) + G\cdot(\vec{T_3}-\vec{T_1}) + H\cdot(\vec{T_2}-\vec{T_1})\times(\vec{T_3}-\vec{T_1}) \tag{1.4.2}
$$

Expanding these vector relations in coordinates, (1.4.2) becomes

$$
\begin{aligned}
X(I) &= (\tfrac{1}{3})(X_1+X_2+X_3) + F\cdot(X_2-X_1) + G\cdot(X_3-X_1)+ \\
&\quad +H\cdot[(Y_2-Y_1)(Z_3-Z_1)-(Y_3-Y_1)(Z_2-Z_1)], \\
Y(I) &= (\tfrac{1}{3})(Y_1+Y_2+Y_3) + F\cdot(Y_2-Y_1) + G\cdot(Z_3-Z_1)+ \\
&\quad +H\cdot[(Z_2-Z_1)(X_3-X_1)-(Z_3-Z_1)(X_2-X_1)], \\
Z(I) &= (\tfrac{1}{3})(Z_1+Z_2+Z_3) + F\cdot(Z_2-Z_1) + G\cdot(Z_3-Z_1)+ \\
&\quad +H\cdot[(X_2-X_1)(Y_3-Y_1)-(X_3-X_1)(Y_2-Y_1)].
\end{aligned}
\tag{1.4.2.1}
$$

The same relations hold with the same constants: F, G, H, independent of whether we have used ground frame coordinates of these four points or have used their ellipsoid or subreflector system coordinates. But we know the coordinates of the four points in the ellipsoid system (equations 1.1 and Table 2), so we can solve directly for F, G, H for each triple T_1, T_2, T_3 of subreflector retrotarget reference points.

To solve (1.4.2.1) we compute the matrices:

$$
[N] = \begin{bmatrix} X(I) - (\frac{1}{3})(X_1+X_2+X_3) \\ Y(I) - (\frac{1}{3})(Y_1+Y_2+Y_3) \\ Z(I) - (\frac{1}{3})(Z_1+Z_2+Z_3) \end{bmatrix}, \tag{1.4.3.1}
$$

$$
[M] = \begin{bmatrix} X_2-X_1 & X_3-X_1 & (Y_2-Y_1)(Z_3-Z_1)-(Y_3-Y_1)(Z_2-Z_1) \\ Y_2-Y_1 & Y_3-Y_1 & (Z_2-Z_1)(X_3-X_1)-(Z_3-Z_1)(X_2-X_1) \\ Z_2-Z_1 & Z_3-Z_1 & (X_2-X_1)(Y_3-Y_1)-(X_3-X_1)(Y_2-Y_1) \end{bmatrix}. \tag{1.4.3.2}
$$

The equation to be solved is then

$$
[N] = [M]\cdot\begin{bmatrix} F \\ G \\ H \end{bmatrix}, \qquad \text{which has the solution} \tag{1.4.3.3}
$$

$$(1.4.4) \qquad \begin{bmatrix} F \\ G \\ H \end{bmatrix} = [M]^{-1} \cdot [N] \ .$$

We determine F, G, H, by substituting for the general coordinates in (1.4.3.1) and (1.4.3.2) the known ellipsoid frame coordinates of the three target reference points. That is, we make the substitutions:

$$\begin{aligned} &X_1 \to X_{ce}(T_1), \quad X_2 \to X_{ce}(T_2), \quad X_3 \to X_{ce}(T_3), \\ (1.4.5) \qquad &Y_1 \to Y_{ce}(T_1), \quad Y_2 \to Y_{ce}(T_2), \quad Y_3 \to Y_{ce}(T_3), \\ &Z_1 \to Z_{ce}(T_1), \quad Z_2 \to Z_{ce}(T_2), \quad Z_3 \to Z_{ce}(T_3), \end{aligned}$$

in equations (1.4.3) and then compute the right side of (1.4.4). The values of F, G, H are tabulated in Table 5 for the various sets of target triple points.

Table 5: Barycentric Coordinates For Subreflector Target Triples.

Target $T_1(A)$	Target $T_2(A)$	Target $T_3(A)$	Triple Index	$F(A)$	$G(A)$	$H(A)$
ZSG305	ZSG316	ZSG317	$A = 01$	−0.1182720	−0.1360649	0.0206087
ZSG312	ZSG321	ZSG313	$A = 02$	−0.3000071	0.1493778	0.0206087
ZSG305	ZSG312	ZSG317	$A = 03$	0.0173785	−0.0493599	0.3112280
ZSG312	ZSG316	ZSG313	$A = 04$	−0.2787017	0.1710119	0.0324327
ZSG316	ZSG321	ZSG305	$A = 05$	−0.0697924	0.3757362	0.0274621
ZSG321	ZSG317	ZSG312	$A = 06$	0.2777942	0.3730633	0.0249293
ZSG317	ZSG313	ZSG316	$A = 07$	0.6133501	0.0997308	0.0278935
ZSG313	ZSG305	ZSG321	$A = 08$	0.4013787	−0.0451674	0.0340463
ZSG305	ZSG312	ZSG321	$A = 09$	−0.2917471	−0.0616690	0.0315572
ZSG312	ZSG316	ZSG317	$A = 10$	−0.7102323	0.0995950	0.0278708
ZSG316	ZSG321	ZSG313	$A = 11$	−0.6465230	0.3783516	0.0244175
ZSG321	ZSG317	ZSG305	$A = 12$	−0.3626068	0.3936161	0.0288911
ZSG317	ZSG313	ZSG312	$A = 13$	0.1072620	0.1713523	0.3254250
ZSG313	ZSG305	ZSG316	$A = 14$	0.0439371	−0.0427824	0.0321185
ZSG305	ZSG312	ZSG313	$A = 15$	0.2260442	0.2299329	0.0526120
ZSG312	ZSG316	ZSG305	$A = 16$	0.3449679	0.7217923	0.0914053
ZSG316	ZSG321	ZSG312	$A = 17$	0.4381853	1.1762942	0.0438282
ZSG321	ZSG317	ZSG316	$A = 18$	0.8185636	0.7889015	0.0450851
ZSG317	ZSG313	ZSG321	$A = 19$	1.2054385	0.4719987	0.0454301
ZSG313	ZSG305	ZSG317	$A = 20$	0.8046592	0.3960635	0.1010776

The computation of coordinates of reference point I by substitution of the coordinates of a measured target triple into (1.4.2.1) is neither a full nor a best solution. It does not use all of the information available from target range measurements and does not properly take into account measurement standard errors of T_1, T_2, T_3. One may possess range measurement adjusted coordinates for more than three subreflector targets (including their adjustment standard errors). If this is so, one may extend the solution procedure, and make use of all available subreflector target coordinate information, in the following way.

Choose three subreflector targets for which adjusted fiducial point measured coordinates are available together with their coordinate standard errors. Obtain approximate coordinates of I by substituting the adjusted coordinates of these three chosen points into (1.4.2.1). Use the coordinate data available for all measured subreflector target fiducial points, together with the approximate coordinates of I just obtained, as input data for approximate coordinates and standard errors for a standard least-squares adjustment routine (for example STAR-NET or GAUSSFIT). Also enter the known distances between pairs of reference points, adjusted for thermal expansion of the subreflector as entry data into the least-squares adjustment routine, along with their standard errors computed in adjustment of the subreflector surface photogrammetry measurements. (The latter adjusted distances have standard error of approximately 0.2 millimeters). Use a moderately large value, a few centimeters for example, as the *a-priori* estimated standard error for the coordinates of I; this is done to avoid a false tight constraint on our prior knowledge of this point's location. Distances between pairs of target reference points and distances between target reference points and point I are known with good accuracy and provide tight constraints on the position of I. The distances have already been computed from the subreflector photogrammetry results (without correction for temperature change and thermal expansion), and are given in Table 2b.

The least-squares adjustment routine's output will include adjusted coordinates for subreflector reference point I and for the prism targets providing input to the adjustment, together with adjustment standard errors.

1.4.2. Determination Of Subreflector Orientation.

We again assume that measured adjusted subreflector frame coordinates are available for three subreflector target reference points: $T_1(A), T_2(A), T_3(A)$, where A is an integer used to index the triples of retrotargets. (The target triples indexes are given in Table 5). We do not assume that the subreflector is at home position. The origin and orientation of the subreflector reference frame are well-defined functions of commanded tipping structure elevation and azimuth only, and do not depend at all upon the location of the subreflector; the subreflector system coordinates of the six retrotarget reference points are determined, however, by the subreflector location relative to home position. We wish, here, to compute the subreflector orientation relative to home position when the subreflector system coordinates are given for the subreflector when off home position. This will be accomplished by providing a rotation matrix, $[\mathcal{R}]$, which specifies the rotation of the subreflector structure when moved from its home position. The three tilt angles of the displaced subreflector as it sits in space can then be found analytically (with some difficulty) from the elements of the rotation matrix $[\mathcal{R}]$.

We directly compute three unit vectors which are obtained from the triple of target points. Corresponding to the target triple indexed by the integer A we define

$$(1.4.6)\quad \hat{t}_{12} = \frac{\hat{T}_2(A) - \hat{T}_1(A)}{\left|\hat{T}_2(A) - \hat{T}_1(A)\right|}, \quad \hat{t}_{13} = \frac{\hat{T}_3(A) - \hat{T}_1(A)}{\left|\hat{T}_3(A) - \hat{T}_1(A)\right|}, \quad \hat{t}_{cp} = \frac{\hat{t}_{12} \times \hat{t}_{13}}{\left|\hat{t}_{12} \times \hat{t}_{13}\right|}.$$

The subreflector system coordinates of these unit vectors can be computed directly from the given subreflector system coordinates of the three chosen target reference points.

As before, we denote the unit basis vectors for the subreflector frame at the commanded elevation and azimuth by $\hat{X}_s$, $\hat{Y}_s$, $\hat{Z}_s$. These basis vectors are related to the basis vectors for the ellipsoid and main reflector reference frames by equations(1.3) and (1.4). Let us assume that copies of these unit vectors are rigidly attached to the subreflector structure at the reference point I_1, when the subreflector is at home position. When the subreflector is moved from home position to an arbitrary commanded position (assuming the commanded tipping structure elevation and azimuth are not changed), the rigidly attached copies of these basis vectors will be translated and rotated. The rotated copies of the subreflector ba-

sis vectors will be related to the original basis vectors by an orthonormal linear transformation. Let this linear transformation be denoted by $\mathcal{R}$ and the rotated basis vectors be denoted by $\mathcal{R}(\hat{X}_s), \mathcal{R}(\hat{Y}_s), \mathcal{R}(\hat{Z}_s)$.

The vectors $\mathcal{R}(\hat{X}_s), \mathcal{R}(\hat{Y}_s), \mathcal{R}(\hat{Z}_s)$ may be expressed as coordinate-independent linear combinations of $\hat{t}_{12}$, $\hat{t}_{13}$, $\hat{t}_{cp}$.

$$
\begin{aligned}
\mathcal{R}\left(\hat{X}_s\right) &= f_{xs} \cdot \hat{t}_{12} + g_{xs} \cdot \hat{t}_{13} + h_{xs} \cdot \hat{t}_{cp}\,, \\
\mathcal{R}\left(\hat{Y}_s\right) &= f_{ys} \cdot \hat{t}_{12} + g_{ys} \cdot \hat{t}_{13} + h_{ys} \cdot \hat{t}_{cp}\,, \\
\mathcal{R}\left(\hat{Z}_s\right) &= f_{zs} \cdot \hat{t}_{12} + g_{zs} \cdot \hat{t}_{13} + h_{zs} \cdot \hat{t}_{cp}\,.
\end{aligned}
\tag{1.4.7}
$$

For each triple of measured subreflector targets, referenced by a value of the index integer A, there are nine scalar constants:
$f_{xs}(A)$, $g_{xs}(A)$, $h_{xs}(A)$, $f_{ys}(A)$, $g_{ys}(A)$, $h_{ys}(A)$, $f_{zs}(A)$, $g_{zs}(A)$, $h_{zs}(A)$,
which can be regarded as elements of a rotation matrix, $[\mathcal{R}]$, which rotates the three target vectors to the subreflector frame basis vector copies which are considered to be embedded in the subreflector structure, and carried along rigidly with it during subreflector movements. That is, we may write:

$$
\begin{bmatrix} \mathcal{R}(\hat{X}_s) \\ \mathcal{R}(\hat{Y}_s) \\ \mathcal{R}(\hat{Z}_s) \end{bmatrix} = \begin{bmatrix} f_{xs} & g_{xs} & h_{xs} \\ f_{ys} & g_{ys} & h_{ys} \\ f_{zs} & g_{zs} & h_{zs} \end{bmatrix} \cdot \begin{bmatrix} \hat{t}_{12} \\ \hat{t}_{13} \\ \hat{t}_{cp} \end{bmatrix} = [\mathcal{R}] \cdot \begin{bmatrix} \hat{t}_{12} \\ \hat{t}_{13} \\ \hat{t}_{cp} \end{bmatrix}. \tag{1.4.8}
$$

The matrix elements may be computed numerically by substituting the values of the vectors $\hat{t}_{12}$, $\hat{t}_{13}$, $\hat{t}_{cp}$ corresponding to subreflector home position as elements in the right side column matrix of (1.4.8) and substituting $\hat{X}_s$, $\hat{Y}_s$, $\hat{Z}_s$ as elements of the left side column matrix. In terms of the subreflector system coordinates of the three targets and their mutual distances one has the following system of three sets of three linear equations to solve for the matrix elements. The coefficients appearing in (1.4.9) are computed using tables 2b and 4 and by computing the subreflector frame components of $\hat{t}_{cp}$ corresponding to the target coordinates when the subreflector is at home position.

$$(1.4.9)\qquad \begin{bmatrix} 1 \\ 0 \\ 0 \end{bmatrix} = \begin{bmatrix} (\hat{t}_{12})_{shp}\cdot\hat{X}_s & (\hat{t}_{13})_{shp}\cdot\hat{X}_s & (\hat{t}_{cp})_{shp}\cdot\hat{X}_s \\ (\hat{t}_{12})_{shp}\cdot\hat{Y}_s & (\hat{t}_{13})_{shp}\cdot\hat{Y}_s & (\hat{t}_{cp})_{shp}\cdot\hat{Y}_s \\ (\hat{t}_{12})_{shp}\cdot\hat{Z}_s & (\hat{t}_{13})_{shp}\cdot\hat{Z}_s & (\hat{t}_{cp})_{shp}\cdot\hat{Z}_s \end{bmatrix} \cdot \begin{bmatrix} f_{xs} \\ g_{xs} \\ h_{xs} \end{bmatrix},$$

$$(1.4.10)\qquad \begin{bmatrix} 0 \\ 1 \\ 0 \end{bmatrix} = \begin{bmatrix} (\hat{t}_{12})_{shp}\cdot\hat{X}_s & (\hat{t}_{13})_{shp}\cdot\hat{X}_s & (\hat{t}_{cp})_{shp}\cdot\hat{X}_s \\ (\hat{t}_{12})_{shp}\cdot\hat{Y}_s & (\hat{t}_{13})_{shp}\cdot\hat{Y}_s & (\hat{t}_{cp})_{shp}\cdot\hat{Y}_s \\ (\hat{t}_{12})_{shp}\cdot\hat{Z}_s & (\hat{t}_{13})_{shp}\cdot\hat{Z}_s & (\hat{t}_{cp})_{shp}\cdot\hat{Z}_s \end{bmatrix} \cdot \begin{bmatrix} f_{ys} \\ g_{ys} \\ h_{ys} \end{bmatrix},$$

$$(1.4.11)\qquad \begin{bmatrix} 0 \\ 0 \\ 1 \end{bmatrix} = \begin{bmatrix} (\hat{t}_{12})_{shp}\cdot\hat{X}_s & (\hat{t}_{13})_{shp}\cdot\hat{X}_s & (\hat{t}_{cp})_{shp}\cdot\hat{X}_s \\ (\hat{t}_{12})_{shp}\cdot\hat{Y}_s & (\hat{t}_{13})_{shp}\cdot\hat{Y}_s & (\hat{t}_{cp})_{shp}\cdot\hat{Y}_s \\ (\hat{t}_{12})_{shp}\cdot\hat{Z}_s & (\hat{t}_{13})_{shp}\cdot\hat{Z}_s & (\hat{t}_{cp})_{shp}\cdot\hat{Z}_s \end{bmatrix} \cdot \begin{bmatrix} f_{zs} \\ g_{zs} \\ h_{zs} \end{bmatrix}.$$

The square matrix on the right side of each equation is inverted and the inverse is multiplied by the column matrix on the left side to give the f, g, h elements. The matrix elements are tabulated numerically in Table 6, for each group of three targets indexed by the integer A. Subreflector-frame components of target-triple vectors $\hat{t}_{12}(A)$, $\hat{t}_{13}(A)$, $\hat{t}_{cp}(A)$ corresponding to the subreflector at home position are listed in table 6b.

The rotated nutation axis is found from the relation

$$(1.4.12)\qquad \mathcal{R}(\hat{X}_{nut}) \;=\; C_s\cdot\mathcal{R}(\hat{X}_s) \;-\; S_s\cdot\mathcal{R}\,(\hat{Y}_s)\,.$$

The rotation matrix elements listed in Table 6 are used in the following manner. We are given a set of measured, least-squares-adjusted coordinates of some of the subreflector prism targets (that is, of their fiducial reference points), in one of the telescope coordinate systems. We wish to find the spatial orientation of the subreflector when these measurements were made. To do this, we first convert these adjusted coordinates to the subreflector system coordinates, using a standard telescope coordinate transformation. We then choose three of the measured

targets and compute vectors $\hat{t}_{12}(A)$, $\hat{t}_{13}(A)$, $\hat{t}_{cp}(A)$ corresponding to this target triple, expressing their components in terms of the basis vectors $\hat{X}_s$, $\hat{Y}_s$, $\hat{Z}_s$ of the subreflector frame. The rotated frame vectors $\mathcal{R}(\hat{X}_s)$, $\mathcal{R}(\hat{Y}_s)$, $\mathcal{R}(\hat{Z}_s)$ which specify the subreflector orientation are computed by substituting into equations (1.4.7) the vectors just computed and the nine corresponding matrix elements tabulated in Table 6.

Table 6: Rotation Matrix Elements For Subreflector Target Triple Vectors.

$T_1(A)$	$T_2(A)$	$T_3(A)$	Index	$f_{xs}(A)$	$g_{xs}(A)$	$h_{xs}(A)$
				$f_{ys}(A)$	$g_{ys}(A)$	$h_{ys}(A)$
				$f_{zs}(A)$	$g_{zs}(A)$	$h_{zs}(A)$
ZSG305	ZSG316	ZSG317	$A = 01$	−0.5950641	−0.5873163	0.1274554
				0.0765718	0.0753698	0.9918443
				−0.9265748	0.9108963	0.0001114
ZSG312	ZSG321	ZSG313	$A = 02$	−1.1239356	0.5233080	0.1073419
				0.1213464	−0.0564240	0.9942222
				−0.0009894	1.0004610	−0.0000748
ZSG305	ZSG312	ZSG317	$A = 03$	−0.5460458	−0.1046140	0.9889080
				0.10533330	0.1046140	0.9889080
				−0.8571475	0.5511972	0.9889080
ZSG312	ZSG316	ZSG313	$A = 04$	−1.0062901	−0.1455913	0.0912475
				0.0922060	0.0134298	0.9958282
				−0.0008831	0.9998726	−0.0000890
ZSG316	ZSG321	ZSG305	$A = 05$	−0.5406781	0.8219911	0.1280913
				0.0705714	−0.1056575	0.9917620
				0.8387957	0.5746300	−0.0008750
ZSG321	ZSG317	ZSG312	$A = 06$	0.4663355	0.8124150	0.1135491
				−0.0639324	−0.0857828	0.9934622
				0.8943272	−0.5949794	0.0118105
ZSG317	ZSG313	ZSG316	$A = 07$	1.0065043	−0.1466201	0.0908144
				−0.0917843	0.0135081	0.9958678
				−0.0007025	−0.9998979	0.0001371

Table 6 (continued)

$T_1(A)$	$T_2(A)$	$T_3(A)$	Index	$f_{xs}(A)$	$g_{xs}(A)$	$h_{xs}(A)$
				$f_{ys}(A)$	$g_{ys}(A)$	$h_{ys}(A)$
				$f_{zs}(A)$	$g_{zs}(A)$	$h_{zs}(A)$
ZSG313	ZSG305	ZSG321	$A = 08$	0.4319887	−0.8326325	0.1276031
				−0.0923497	0.0837904	0.9909677
				−0.8825436	−0.5629287	−0.0412359
ZSG305	ZSG312	ZSG321	$A = 09$	−0.0051510	−0.9889158	0.1283744
				0.0503319	0.1011249	0.9909046
				−1.2196702	0.6628702	0.0403493
ZSG312	ZSG316	ZSG317	$A = 10$	−0.9353200	−0.1525366	0.0912146
				0.0857391	0.0138279	0.9958312
				−0.4882326	1.0474192	0.0001368
ZSG316	ZSG321	ZSG313	$A = 11$	−0.9960385	0.9240050	0.1129583
				0.1192453	−0.0976384	0.9935339
				0.5213506	0.6440497	−0.0114385
ZSG321	ZSG317	ZSG305	$A = 12$	0.0113682	0.9850689	0.1281101
				−0.0028698	−0.1264207	0.9917593
				1.2287566	−0.7235405	0.0011310
ZSG317	ZSG313	ZSG312	$A = 13$	1.0900539	−0.1789874	0.0907812
				−0.0993156	0.0162065	0.9958709
				0.5689743	−1.2204563	−0.0000894
ZSG313	ZSG305	ZSG316	$A = 14$	0.9763086	−0.9366170	0.1459994
				−0.1590694	0.1197698	0.9888664
				−0.5130211	−0.6364718	−0.0287667

Table 6 (continued).

$T_1(A)$	$T_2(A)$	$T_3(A)$	Index	$f_{xs}(A)$	$g_{xs}(A)$	$h_{xs}(A)$
				$f_{ys}(A)$	$g_{ys}(A)$	$h_{ys}(A)$
				$f_{zs}(A)$	$g_{zs}(A)$	$h_{zs}(A)$
ZSG305	ZSG312	ZSG313	$A = 15$	−0.8979189	−0.8624361	0.1880782
				0.1719455	0.1651546	0.9821541
				−0.6174309	0.5877798	−0.0000032
ZSG312	ZSG316	ZSG305	$A = 16$	−1.1203275	−0.2064314	0.0804702
				0.0368199	−0.0817525	0.9941351
				0.7411683	1.3548145	0.0722495
ZSG316	ZSG321	ZSG312	$A = 17$	−0.1583171	0.9149809	0.0947209
				0.0418398	−0.0716773	0.9952114
				1.1042621	0.6355171	−0.0241279
ZSG321	ZSG317	ZSG316	$A = 18$	0.8627946	0.8486029	0.1295000
				−0.1127477	−0.1107582	0.9915794
				0.6033200	−0.6234800	0.0001100
ZSG317	ZSG313	ZSG321	$A = 19$	0.9104377	−0.1610968	0.0945339
				−0.0693233	0.0441517	0.9951896
				−0.6642349	−1.1166955	0.0257099
ZSG313	ZSG305	ZSG317	$A = 20$	−0.2000201	−1.1225552	0.0797877
				−0.0801118	0.0348302	0.9941094
				−1.3033097	−0.7490155	−0.0733509

Table 6b: Home Position Components Of Target Triple Vectors.

$T_1(A)$	$T_2(A)$	$T_3(A)$	Index	$(\hat{t}_{12})_{hp} \cdot \hat{X}_s$	$(\hat{t}_{12})_{hp} \cdot \hat{Y}_s$	$(\hat{t}_{12})_{hp} \cdot \hat{Z}_s$
				$(\hat{t}_{13})_{hp} \cdot \hat{X}_s$	$(\hat{t}_{13})_{hp} \cdot \hat{Y}_s$	$(\hat{t}_{13})_{hp} \cdot \hat{Z}_s$
				$(\hat{t}_{cp})_{hp} \cdot \hat{X}_s$	$(\hat{t}_{cp})_{hp} \cdot \hat{Y}_s$	$(\hat{t}_{cp})_{hp} \cdot \hat{Z}_s$
ZSG305	ZSG316	ZSG317	$A = 01$	−0.8249516	0.1060698	−0.5406785
				−0.8391664	0.1077742	0.5478351
				0.1274554	0.9918443	0.0001114
ZSG312	ZSG321	ZSG313	$A = 02$	−0.8798803	0.0950320	0.4655958
				−0.0008622	0.0001684	0.9999996
				0.1073419	0.9942222	−0.0000748
ZSG305	ZSG312	ZSG317	$A = 03$	−0.5347570	0.1024010	−0.8134096
				−0.8391664	0.1077742	0.5478351
				0.1457327	0.9889080	0.0286861
ZSG312	ZSG316	ZSG313	$A = 04$	−0.9853504	0.0902745	−0.1446893
				−0.0008622	0.0001684	0.9999996
				0.0912745	0.9958282	−0.0000890
ZSG316	ZSG321	ZSG305	$A = 05$	−0.5650122	0.0736993	0.8217844
				0.8249516	−0.1060698	0.5406785
				0.1280913	0.9917620	−0.0008750
ZSG321	ZSG317	ZSG312	$A = 06$	0.5838686	−0.0763427	0.8082507
				0.8798803	−0.0950320	−0.4655958
				0.1135491	0.9934622	0.0118105
ZSG317	ZSG313	ZSG316	$A = 07$	0.9852448	−0.0898256	−0.1456850
				−0.0006798	0.0001997	−0.9999997
				0.0908144	0.9958678	0.0001371

Table 6b (continued)

$T_1(A)$	$T_2(A)$	$T_3(A)$	Index	$(\hat{t}_{12})_{hp} \cdot \hat{X}_s$	$(\hat{t}_{12})_{hp} \cdot \hat{Y}_s$	$(\hat{t}_{12})_{hp} \cdot \hat{Z}_s$
				$(\hat{t}_{13})_{hp} \cdot \hat{X}_s$	$(\hat{t}_{13})_{hp} \cdot \hat{Y}_s$	$(\hat{t}_{13})_{hp} \cdot \hat{Z}_s$
				$(\hat{t}_{cp})_{hp} \cdot \hat{X}_s$	$(\hat{t}_{cp})_{hp} \cdot \hat{Y}_s$	$(\hat{t}_{cp})_{hp} \cdot \hat{Z}_s$
ZSG313	ZSG305	ZSG321	$A = 08$	0.5617322	−0.1075720	−0.8468747
				−0.8900151	0.0969576	−0.4456973
				0.1276031	0.9909677	−0.0412359
ZSG305	ZSG312	ZSG321	$A = 09$	−0.5347570	0.1024010	−0.8134096
				−0.9917583	0.1280992	0.0094747
				0.1283744	0.9909046	0.0403493
ZSG312	ZSG316	ZSG317	$A = 10$	−0.9853504	0.0902745	−0.1446893
				−0.4593125	0.0419495	0.8872837
				0.0912146	0.9958312	0.0001368
ZSG316	ZSG321	ZSG313	$A = 11$	−0.5650122	0.0736993	0.8217844
				0.4593768	−0.0420133	0.8872473
				0.1129583	0.9935339	−0.0114385
ZSG321	ZSG317	ZSG305	$A = 12$	0.5838686	−0.0763427	0.8082507
				0.9917583	−0.1280992	−0.0094747
				0.1281101	0.9917593	0.0011310
ZSG317	ZSG313	ZSG312	$A = 13$	0.9852448	−0.0898256	−0.145685
				0.4593125	−0.0419495	−0.8872837
				0.0907812	0.9958709	−0.0000894
ZSG313	ZSG305	ZSG316	$A = 14$	0.5617322	−0.1075720	−0.8468747
				−0.4593768	0.0420133	−0.8872473
				0.1459994	0.9888664	−0.0287667

Table 6b (continued).

$T_1(A)$	$T_2(A)$	$T_3(A)$	Index	$(\hat{t}_{12})_{hp} \cdot \hat{X}_s$	$(\hat{t}_{12})_{hp} \cdot \hat{Y}_s$	$(\hat{t}_{12})_{hp} \cdot \hat{Z}_s$
				$(\hat{t}_{13})_{hp} \cdot \hat{X}_s$	$(\hat{t}_{13})_{hp} \cdot \hat{Y}_s$	$(\hat{t}_{13})_{hp} \cdot \hat{Z}_s$
				$(\hat{t}_{cp})_{hp} \cdot \hat{X}_s$	$(\hat{t}_{cp})_{hp} \cdot \hat{Y}_s$	$(\hat{t}_{cp})_{hp} \cdot \hat{Z}_s$
ZSG305	ZSG312	ZSG313	$A = 15$	−0.5347570	0.1024010	−0.8134096
				−0.5617322	0.1075720	0.8468747
				0.1880782	0.9821541	−0.0000032
ZSG312	ZSG316	ZSG305	$A = 16$	−0.9853504	0.0902745	−0.1446893
				0.5347570	−0.1024010	0.8134096
				0.0804702	0.9941351	0.0722495
ZSG316	ZSG321	ZSG312	$A = 17$	−0.5650122	0.0736993	0.8217844
				0.9853504	−0.0902745	0.1446893
				0.0947209	0.9952114	−0.0241279
ZSG321	ZSG317	ZSG316	$A = 18$	0.5838686	−0.0763427	0.8082507
				0.5650122	−0.0736993	−0.8217844
				0.1295000	0.9915794	0.0001100
ZSG317	ZSG313	ZSG321	$A = 19$	0.9852448	−0.0898256	−0.1456850
				−0.5838686	0.0763427	−0.8082507
				0.0945339	0.9951896	0.0257099
ZSG313	ZSG305	ZSG317	$A = 20$	0.5617322	−0.1075720	−0.8468747
				−0.9852448	0.0898256	0.1456850
				0.0797877	0.9941094	−0.0733509

1.5. Rangefinder Aiming

The metrology problem to be solved here is the following. The subreflector is not at home position. A position and orientation of the subreflector are assumed to be commanded with respect to the ground, and specified by a message stating the tipping structure azimuth and elevation and the six local subreflector parameters. The present task is to compute local rangefinder aiming coordinates (with respect to the appropriate rangefinder support platforms) to aim a ground-based or feed arm rangefinder to the reference point of a subreflector prism range target. We will be able to achieve rangefinder aiming if we are able to compute the coordinates of the subreflector's retrotarget reference points with respect to the ground reference frame. (We can for example convert these subsequently to main reflector frame coordinates). Computational algorithms already exist to specify the locations and orientations of the rangefinders. What remains, is to specify the spatial locations of the subreflector target reference points.

For the purpose of aiming the rangefinders, the location of the subreflector retrotarget reference points will have to be computed as functions of eight independent variables: commanded tipping structure elevation and azimuth, three subreflector offset angles from home position and three subreflector displacements from home position. These are specified by the subreflector state vector, S. To compute target point locations, the subreflector ellipsoid center point coordinates and ellipsoid axis direction cosines will have to be computed as functions of these independent variables, for a geometric design telescope. That is the rangefinders are aimed to points in space specified by a geometric telescope model. The components of the state vector S are considered to be setpoint values for a geometric telescope; the modalities for actually driving the subreflector to this location do not have to be considered here. But feed arm rangefinder platform orientations and locations will have to be found using the telescope's Finite Element Model, because gravity deformation of the telescope affects the relative locations and orientations of the feed arm rangefinders with respect to the feed arm tip, and consequently affects rangefinder locations with respect to the subreflector, even at home position.

Ellipsoid frame coordinates of the fiducial point of each subreflector structure

target j (listed in Table 2) were computed from the known geometry of the prism installation into the subreflector structure. GBT Archives Drawing D35420M200 [Taggart-1] defines the prism installation geometry. When ground frame coordinates of three (or preferably four) subreflector prism target fiducial reference points are provided, the ground frame coordinates of the ellipsoid center can be calculated, and the direction cosines of the ellipsoid frame unit basis vectors relative to the ground frame can also be computed. These coordinates and direction cosines are computed for a general case where the subreflector has known angular and distance displacements from its home position relative to the subreflector reference frame. The subreflector frame has, presently, only been defined with respect to a geometric model of the GBT. It has been conceived, to date, only within the paradigm of a telescope consisting of a rigid alidade linked to a rigid tipping structure. It has not yet been defined for an elastically deformable telescope, possessing subreflector actuators pinned to the end of a flexible feed arm.

We are thereby presented with the following real problem. By using rangefinder metrology we can locate the current position and orientation of the subreflector with respect to the ground. The subreflector is moved by resetting the lengths of six Stewart Platform piston actuators, which give it known displacements and tilts with respect to the tip of the telescope feed arm (which is a flexible cantilever). To control the subreflector position with respect to the main reflector and the physical Gregorian focus at the receiver room horn flange, the position and orientation of the subreflector will have to be located with respect to the ground reference frame. This could be done in the following way.

When the independent subreflector variables are specified by calling out S in a (Gregorian) Focus Tracking Synchronization Message, one is given enough information to calculate displacement components of the subreflector ellipsoid's center point and optical axis reference point from their home positions, and also to compute the direction cosines of the unit vectors along the ellipsoid axes (which are tilted, for non-zero values of the six independent subreflector variables) with respect to the ellipsoid unit basis vectors at home position. We compute the subreflector position and orientation with respect to ground for home position, given the subreflector state vector, S. After computing the subreflector position and orientation for subreflector home position, we can subsequently specify subreflector position and orientation with respect to ground, for an arbitrary given set of values for the six independent subreflector variables, and compute the retro-

target reference point coordinates to aim at. The computations are given in the paragraphs which follow.

When the subreflector is at home position, for a geometric telescope at commanded elevation EL_{com} and commanded azimuth AZ_{com} the ground frame coordinates of the subreflector prism target fiducial points are given by:

$$(2.1.1a) \qquad \begin{bmatrix} X(T_j) \\ Y(T_j) \\ Z(T_j) \end{bmatrix}_{hp} = \begin{bmatrix} X(I_1) \\ Y(I_1) \\ Z(I_1) \end{bmatrix}_{hp} + [R71] \begin{bmatrix} X_{ce}(T_j) - X_{ce}(I_1) \\ Y_{ce}(T_j) - Y_{ce}(I_1) \\ Z_{ce}(T_j) - Z_{ce}(I_1) \end{bmatrix}_{hp}, \text{ or}$$

$$(2.1.1b) \qquad \begin{bmatrix} X(T_j) \\ Y(T_j) \\ Z(T_j) \end{bmatrix}_{hp} = \begin{bmatrix} X(I_1) \\ Y(I_1) \\ Z(I_1) \end{bmatrix}_{hp} + [R71] \begin{bmatrix} \delta_{xj} \\ \delta_{yj} \\ \delta_{zj} \end{bmatrix}.$$

The values of δ_{xj}, δ_{yj}, δ_{zj} are constants which are computed by subtracting the ellipsoid system coordinates of I_1 given in equations (1.1) from those of the subreflector targets, given in Table 2. The subscript "*hp*" denotes values computed for the subreflector home position. The column vector of ground frame coordinates for the reference point I_1 at home position (corresponding to commanded telescope angles) is computed from the geometric telescope design geometry, and turns out to be

$$(2.1.2) \qquad \begin{bmatrix} X(I_1) \\ Y(I_1) \\ Z(I_1) \end{bmatrix}_{hp} = \begin{bmatrix} T16 \end{bmatrix} =$$

$$= \begin{bmatrix} (\sin AZ_{com} \cdot \sin EL_{com} \cdot d_{se}) - (\sin AZ_{com} \cdot \cos EL_{com} \cdot h_{se}) \\ (\cos AZ_{com} \cdot \sin EL_{com} \cdot d_{se}) - (\cos AZ_{com} \cdot \cos EL_{com} \cdot h_{se}) \\ (\cos EL_{com} \cdot d_{se}) - (\sin EL_{com} \cdot h_{se}) \end{bmatrix}.$$

The lengths d_{se} and h_{se} are given, for the geometric design telescope, in Appendix I of [Goldman-1], and have the values:

$$(2.1.2b) \qquad d_{se} = 62.731110 \text{ meters}, \qquad h_{se} = 69.291990 \text{ meters}.$$

In terms of the commanded telescope elevation and azimuth angles, the coordinate rotation matrix $[R71(az(t), el(t))]$ from the ellipsoid reference frame to the

ground reference frame is:

(2.1.3) $[R71] =$

$$\begin{bmatrix} 0 & S_\beta & C_\beta \\ 0 & -C_\beta & S_\beta \\ 1 & 0 & 0 \end{bmatrix} \begin{bmatrix} \cos AZ_{com} & -\sin AZ_{com} & 0 \\ (\sin AZ_{com} \cdot \sin EL_{com}) & (\cos AZ_{com} \cdot \sin EL_{com}) & -\cos EL_{com} \\ (\sin AZ_{com} \cdot \cos EL_{com}) & (\cos AZ_{com} \cdot \cos EL_{com}) & \sin EL_{com} \end{bmatrix} .$$

We can now compute the positions of the subreflector target reference point locations corresponding to a subreflector at a commanded position specified by the subreflector state vector S. We compute these coordinates in the subreflector coordinate system. They can subsequently be transformed into coordinates in other telescope coordinate systems using coordinate transformations which are already available. See e.g. Appendix I of [Goldman-1].

1.5.1. Coordinates Of Subreflector Retrotarget Reference Points.

We now compute the subreflector system coordinates of reference point T_j of subreflector retrotarget j, when the subreflector is at the general position specified by state vector S. We begin by considering the coordinates of T_j when the subreflector is at home position state $S_{hp}(AZ_{com}, EL_{com})$. The home position subreflector system coordinates of T_j are denoted by the symbols

$$X_{shp}(T_j) \quad , \quad Y_{shp}(T_j) \quad , \quad Z_{shp}(T_j) \, .$$

These coordinates are constants; their numerical values appear in Table 4.

In terms of these coordinates, the displacement vector from subreflector reference point I_1 to target reference point T_j is:

(2.2.1) $$\vec{X}_{shp}(T_j) \; = \; X_{shp}(T_j) \cdot \hat{X}_s + Y_{shp}(T_j) \cdot \hat{Y}_s + Z_{shp}(T_j) \cdot \hat{Z}_s \quad ,$$

where $\hat{X}_s \, , \hat{Y}_s \, , \hat{Z}_s$ are the subreflector frame basis vectors when the subreflector is at home position $S_{hp}(AZ_{com}, EL_{com})$.

We use the notation:

(2.2.2) $$\mathcal{R} \; = \; \mathcal{R}_3(\theta_z \cdot \hat{Z}_s) \cdot \mathcal{R}_2(\theta_y \cdot \hat{Y}_s) \cdot \mathcal{R}_1(\theta_{nut} \cdot \hat{X}_{nut})$$

to denote the operation of rotating the subreflector successively by the (radian) angles θ_{nut} about the subreflector nutation axis, θ_y about the subreflector Y_s-axis, and θ_z about the subreflector Z_s-axis, while leaving reference point I_1 fixed in position. By convention these are right-handed rotations when these angles are positive.

After the subreflector is moved to the position specified by state vector S, the target reference point T_j will have moved to the position given by the displacement vector

$$(2.3.2) \qquad \vec{T}_j(\mathrm{S}) = X_s(I)\cdot\hat{X}_s + Y_s(I)\cdot\hat{Y}_s + Z_s(I)\cdot\hat{Z}_s + \mathcal{R}\left[\vec{X}_{shp}(T_j)\right] .$$

Because the rotation operator is linear when acting on the sum of displacement vectors we get,

$$(2.3.3) \quad \mathcal{R}\left[\vec{X}_{shp}(T_j)\right] = X_{shp}(T_j)\cdot\mathcal{R}\left[\hat{X}_s\right] + Y_{shp}(T_j)\cdot\mathcal{R}\left[\hat{Y}_s\right] + Z_{shp}(T_j)\cdot\mathcal{R}\left[\hat{Z}_s\right] .$$

$$(2.3.4) \quad \vec{T}_j(\mathrm{S}) = X_s(I)\cdot\hat{X}_s + Y_s(I)\cdot\hat{Y}_s + Z_s(I)\cdot\hat{Z}_s + X_{shp}(T_j)\cdot\mathcal{R}\left[\hat{X}_s\right] +$$
$$+Y_{shp}(T_j)\cdot\mathcal{R}\left[\hat{Y}_s\right] + Z_{shp}(T_j)\cdot\mathcal{R}\left[\hat{Z}_s\right] .$$

We use the notation:

$$(2.3.5) \qquad \vec{T}_j(\mathrm{S}) = X_{sj}\cdot\hat{X}_s + Y_{sj}\cdot\hat{Y}_s + Z_{sj}\cdot\hat{Z}_s$$

to denote the displacement of $T_j(\mathrm{S})$ from the origin point I_1 of the subreflector. Here,

X_{sj} is the $\hat{X}_s$-component of $\vec{T}_j(\mathrm{S})$,
Y_{sj} is the $\hat{Y}_s$-component of $\vec{T}_j(\mathrm{S})$,
Z_{sj} is the $\hat{Z}_s$-component of $\vec{T}_j(\mathrm{S})$.

To compute the part of the retrotarget displacements caused by subreflector rotations about the reference point I we use the following result of classical vector analysis. (See e.g. H. Goldstein's Classical Mechanics).

Given a displacement vector $\vec{v}$ from a point I we wish to rotate $\vec{v}$ about an axis through I by a right-hand rotation angle θ so that the (oriented) axis of rotation points along the direction of a unit vector $\hat{u}$. Calling $\vec{v}'$ the rotated vector we may write in symbolic notation $\vec{v} \to \vec{v}'$ or

$$\mathcal{R}(\theta \cdot \hat{u})\,[\vec{v}] \;=\; \vec{v}\,' \,. \tag{2.3.6}$$

It can be shown that the rotation may be computed explicitly using the formula

$$\vec{v}' \;=\; (\hat{u})(\hat{u}\cdot\vec{v})(1-\cos\theta) + (\vec{v})\cos\theta + (\hat{u}\times\vec{v})\sin\theta \,. \tag{2.3.7}$$

We use this formula to compute the rotated vectors appearing in (2.3.2) and (2.3.4). We will use the abbreviations:

$$\begin{array}{lll} C_n = \cos\theta_{nut} & , & S_n = \sin\theta_{nut} \,, \\ C_y = \cos\theta_y & , & S_y = \sin\theta_y \quad , \\ C_z = \cos\theta_z & , & S_z = \sin\theta_z \quad . \end{array} \tag{2.3.8}$$

We now compute the rotated vectors. First we rotate $\hat{X}_s$ by θ_{nut} about $\hat{X}_{nut}$. Equation (2.3.7) gives

$$\mathcal{R}_1\left[\hat{X}_s\right] \;=\; (\hat{X}_{nut})(\hat{X}_{nut}\cdot\hat{X}_s)(1-C_n) \;+ \tag{2.3.8}$$

$$+\; (\hat{X}_s)(C_n) \;+\; (\hat{X}_{nut}\times\hat{X}_s)(S_n)\,, \qquad \text{and}$$

$$\mathcal{R}_1\left[\hat{X}_s\right] \;=\; (C_s\cdot\hat{X}_s - S_s\cdot\hat{Y}_s)(C_s)(1-C_n) \;+ \tag{2.3.8b}$$

$$+\,(\hat{X}_s)(C_n) \;+ \begin{vmatrix} \hat{X}_s & \hat{Y}_s & \hat{Z}_s \\ C_s & -S_s & 0 \\ 1 & 0 & 0 \end{vmatrix} (S_n)\,, \quad \text{which gives,}$$

$$\mathcal{R}_1\left[\hat{X}_s\right] \;=\; (C_s^2 + S_s^2\cdot C_n)\hat{X}_s + (-C_s\cdot S_s)(1-C_n)\hat{Y}_s + (S_s\cdot S_n)\hat{Z}_s \,. \tag{2.3.9a}$$

By similar computations we get rotations of $\hat{Y}_s$ and $\hat{Z}_s$ by θ_{nut} about $\hat{X}_{nut}$,

$$\mathcal{R}_1\left[\hat{Y}_s\right] \;=\; (-C_s\cdot S_s)(1-C_n)\hat{X}_s + (S_s^2 + C_s^2\cdot C_n)\hat{Y}_s + (C_s\cdot S_n)\hat{Z}_s \,, \tag{2.3.9b}$$

$$\mathcal{R}_1\left[\hat{Z}_s\right] \;=\; (-S_s\cdot S_n)\hat{X}_s + (-C_s\cdot S_n)\hat{Y}_s + (C_n)\hat{Z}_s \,. \tag{2.3.9c}$$

These results can be written as

$$(2.3.10) \qquad \mathcal{R}_1 \begin{bmatrix} \hat{X}_s \\ \hat{Y}_s \\ \hat{Z}_s \end{bmatrix} =$$

$$\begin{bmatrix} (C_s^2 + S_s^2 \cdot C_n) & (-C_s \cdot S_s)(1 - C_n) & (S_s \cdot S_n) \\ (-C_s \cdot S_s)(1 - C_n) & (S_s^2 + C_s^2 \cdot C_n) & (C_s \cdot S_n) \\ (-S_s \cdot S_n) & (-C_s \cdot S_n) & (C_n) \end{bmatrix} \cdot \begin{bmatrix} \hat{X}_s \\ \hat{Y}_s \\ \hat{Z}_s \end{bmatrix} \quad \text{or}$$

$$(2.3.11) \quad \mathcal{R}_1 \begin{bmatrix} \hat{X}_s \\ \hat{Y}_s \\ \hat{Z}_s \end{bmatrix} = \begin{bmatrix} A_{11} & A_{12} & A_{13} \\ A_{21} & A_{22} & A_{23} \\ A_{31} & A_{32} & A_{33} \end{bmatrix} \cdot \begin{bmatrix} \hat{X}_s \\ \hat{Y}_s \\ \hat{Z}_s \end{bmatrix} = [A] \cdot \begin{bmatrix} \hat{X}_s \\ \hat{Y}_s \\ \hat{Z}_s \end{bmatrix} \quad \text{where}$$

$$(2.3.12) \quad \begin{array}{lll} A_{11} = (C_s^2 + S_s^2 \cdot C_n) & A_{12} = (-C_s \cdot S_s)(1 - C_n) & A_{13} = (S_s \cdot S_n) \\ A_{21} = (-C_s \cdot S_s)(1 - C_n) & A_{22} = (S_s^2 + C_s^2 \cdot C_n) & A_{23} = (C_s \cdot S_n) \\ A_{31} = (-S_s \cdot S_n) & A_{32} = (-C_s \cdot S_n) & A_{33} = (C_n) \ . \end{array}$$

It can be verified that rotation matrix $[A]$ is an orthonormal matrix. Its elements are computed explicitly from trigonometric functions of $\theta_s = 36.7°$ and θ_{nut}.

We next rotate $\mathcal{R}_1 \left[\hat{X}_s\right], \mathcal{R}_1 \left[\hat{Y}_s\right], \mathcal{R}_1 \left[\hat{Z}_s\right]$ by $\mathcal{R}_2(\theta_y \cdot \hat{Y}_s)$. Using (2.3.7) again, we get,

$$(2.3.13) \quad \mathcal{R}_2\mathcal{R}_1 \left[\hat{X}_s\right] = (\hat{Y}_s)(\hat{Y}_s \cdot (A_{11}\hat{X}_s + A_{12}\hat{Y}_s + A_{13}\hat{Z}_s))(1 - C_y) +$$

$$+ (A_{11}\hat{X}_s + A_{12}\hat{Y}_s + A_{13}\hat{Z}_s)(C_y) + \begin{vmatrix} \hat{X}_s & \hat{Y}_s & \hat{Z}_s \\ 0 & 1 & 0 \\ A_{11} & A_{12} & A_{13} \end{vmatrix} (S_y), \quad \text{reducing to}$$

$$(2.3.13b) \quad \mathcal{R}_2\mathcal{R}_1 \left[\hat{X}_s\right] = \hat{X}_s(A_{11}C_y + A_{13}S_y) + \hat{Y}_s(A_{12}) + \hat{Z}_s(A_{13}C_y - A_{11}S_y) \ .$$

Similar manipulations give

$$(2.3.14) \quad \mathcal{R}_2\mathcal{R}_1 \left[\hat{Y}_s\right] = \hat{X}_s(A_{21}C_y + A_{23}S_y) + \hat{Y}_s(A_{22}) + \hat{Z}_s(A_{23}C_y - A_{21}S_y) \ .$$

$$(2.3.15)\quad \mathcal{R}_2\mathcal{R}_1\left[\hat{Z}_s\right] = \hat{X}_s(A_{31}C_y + A_{33}S_y) + \hat{Y}_s(A_{32}) + \hat{Z}_s(A_{33}C_y - A_{31}S_y)\ .$$

Results (2.3.13) through (2.3.15) can be written as

$$(2.3.16)\quad \mathcal{R}_2\mathcal{R}_1\begin{bmatrix}\hat{X}_s\\ \hat{Y}_s\\ \hat{Z}_s\end{bmatrix} = \begin{bmatrix}B_{11} & B_{12} & B_{13}\\ B_{21} & B_{22} & B_{23}\\ B_{31} & B_{32} & B_{33}\end{bmatrix}\cdot\begin{bmatrix}\hat{X}_s\\ \hat{Y}_s\\ \hat{Z}_s\end{bmatrix} = [B]\cdot\begin{bmatrix}\hat{X}_s\\ \hat{Y}_s\\ \hat{Z}_s\end{bmatrix} \quad \text{where}$$

$$(2.3.17)\quad \begin{array}{lll} B_{11} = A_{11}C_y + A_{13}S_y & B_{12} = A_{12} & B_{13} = A_{13}C_y - A_{11}S_y\\ B_{21} = A_{21}C_y + A_{23}S_y & B_{22} = A_{22} & B_{23} = A_{23}C_y - A_{21}S_y\\ B_{31} = A_{31}C_y + A_{33}S_y & B_{32} = A_{32} & B_{33} = A_{33}C_y - A_{31}S_y\ . \end{array}$$

Numerical values for elements of $[B]$ are computed explicitly from trigonometric functions of θ_y and previously computed elements of $[A]$.

Finally, we rotate $\mathcal{R}_2\mathcal{R}_1\left[\hat{X}_s\right]$, $\mathcal{R}_2\mathcal{R}_1\left[\hat{Y}_s\right]$, $\mathcal{R}_2\mathcal{R}_1\left[\hat{Z}_s\right]$ by $\mathcal{R}_3(\theta_z\cdot\hat{Z}_s)$. We get

$$(2.3.18)\quad \mathcal{R}\left[\hat{X}_s\right] = (\hat{Z}_s)(\hat{Z}_s\cdot(B_{11}\hat{X}_s + B_{12}\hat{Y}_s + B_{13}\hat{Z}_s))(1-C_z) +$$

$$+ (B_{11}\hat{X}_s + B_{12}\hat{Y}_s + B_{13}\hat{Z}_s)(C_z) + \begin{vmatrix}\hat{X}_s & \hat{Y}_s & \hat{Z}_s\\ 0 & 0 & 1\\ B_{11} & B_{12} & B_{13}\end{vmatrix}(S_z)\,, \quad \text{reducing to}$$

$$(2.3.18b)\quad \mathcal{R}\left[\hat{X}_s\right] = \hat{X}_s(B_{11}C_z - B_{12}S_z) + \hat{Y}_s(B_{12}C_z + B_{11}S_z) + \hat{Z}_s(B_{13})\ .$$

Similar manipulations give

$$(2.3.19)\quad \mathcal{R}\left[\hat{Y}_s\right] = \hat{X}_s(B_{21}C_z - B_{22}S_z) + \hat{Y}_s(B_{22}C_z + B_{21}S_z) + \hat{Z}_s(B_{23})\ .$$

$$(2.3.20)\quad \mathcal{R}\left[\hat{Z}_s\right] = \hat{X}_s(B_{31}C_z - B_{32}S_z) + \hat{Y}_s(B_{32}C_z + B_{31}S_z) + \hat{Z}_s(B_{33})\ .$$

Results (2.3.18) through (2.3.20) can be written as

$$(2.3.21)\quad \mathcal{R}\begin{bmatrix}\hat{X}_s\\ \hat{Y}_s\\ \hat{Z}_s\end{bmatrix} = \begin{bmatrix}D_{11} & D_{12} & D_{13}\\ D_{21} & D_{22} & D_{23}\\ D_{31} & D_{32} & D_{33}\end{bmatrix}\cdot\begin{bmatrix}\hat{X}_s\\ \hat{Y}_s\\ \hat{Z}_s\end{bmatrix} = [D]\cdot\begin{bmatrix}\hat{X}_s\\ \hat{Y}_s\\ \hat{Z}_s\end{bmatrix} \quad \text{where}$$

$$(2.3.22)\quad \begin{array}{lll} D_{11} = B_{11}C_z - B_{12}S_z & D_{12} = B_{12}C_z + B_{11}S_z & D_{13} = B_{13}\\ D_{21} = B_{21}C_z - B_{22}S_z & D_{22} = B_{22}C_z + B_{21}S_z & D_{23} = B_{23}\\ D_{31} = B_{31}C_z - B_{32}S_z & D_{32} = B_{32}C_z + B_{31}S_z & D_{33} = B_{33}\,. \end{array}$$

Numerical values for elements of $[D]$ are computed explicitly from trigonometric functions of θ_z and previously computed elements of $[B]$. We have now obtained the rotated basis vectors needed to compute the displacement vector $\vec{T}_j(\mathrm{S})$. Inserting the rotated basis vectors given in (2.3.21) into (2.3.4) we get

$$(2.3.22)\quad \begin{bmatrix}T_{jx}(\mathrm{S})\\ T_{jy}(\mathrm{S})\\ T_{jz}(\mathrm{S})\end{bmatrix} = \begin{bmatrix}X_s(I)\\ Y_s(I)\\ Z_s(I)\end{bmatrix} + [D]^{Tr}\cdot\begin{bmatrix}X_{shp}(T_j)\\ Y_{shp}(T_j)\\ Z_{shp}(T_j)\end{bmatrix}.$$

Our final results are, for the individual coordinates of target point T_j, in the subreflector coordinate system:

(2.3.22)

$$T_{jx}(\mathrm{S}) = X_s(I) + X_{shp}(T_j)\cdot D_{11} + Y_{shp}(T_j)\cdot D_{21} + Z_{shp}(T_j)\cdot D_{31}\,,$$

$$T_{jy}(\mathrm{S}) = Y_s(I) + X_{shp}(T_j)\cdot D_{12} + Y_{shp}(T_j)\cdot D_{22} + Z_{shp}(T_j)\cdot D_{32}\,,$$

$$T_{jz}(\mathrm{S}) = Z_s(I) + X_{shp}(T_j)\cdot D_{13} + Y_{shp}(T_j)\cdot D_{23} + Z_{shp}(T_j)\cdot D_{33}\,.$$

By converting these target reference point coordinates from the subreflector coordinate system to the ground coordinate system we obtain the aiming coordinates for ground based rangefinders for subreflector targets. If we convert these subreflector target point coordinates to the main reflector coordinate system we can compute aiming points for the feed arm rangefinders, whose platform positions and orientations are also referenced to the main reflector coordinate system. The target fiducial point home position subreflector system coordinates appearing in (2.3.22) are listed in Table 4.

1.5.2. Subreflector Target Prism Axis Directions.

The direction cosines of the subreflector target prism axes with respect to the subreflector reference frame basis vectors can be calculated by the methods of the previous section, for the case where the subreflector has been positioned to correspond to the state vector S. To do this one starts with the known and tabulated direction cosines of the prism axis unit vector in the ellipsoid system. One next expresses the unit vector $\hat{N}_j$ directed along the axis of target prism j in terms of its subreflector system coordinates: N^{hp}_{xsj}, N^{hp}_{ysj}, N^{hp}_{zsj}, computed for the case that the subreflector is at its home position $S_{hp}(Az_{com}, EL_{com})$. We then rotate the prism axis vector to correspond to state vector S using the method of the previous section.

Using (1.7.1) and (1.3) we can express the unit vector directed along the axis of target prism j , when the subreflector is at home position, in terms of subreflector frame basis vectors.

$$(2.4.1)\quad \hat{N}_j = \begin{bmatrix} N_{xce} & N_{yce} & N_{zce} \end{bmatrix} \cdot \begin{bmatrix} S_{sce} & C_{sce} & 0 \\ -C_{sce} & S_{sce} & 0 \\ 0 & 0 & 1 \end{bmatrix} \cdot \begin{bmatrix} \hat{X}_s \\ \hat{Y}_s \\ \hat{Z}_s \end{bmatrix} .$$

When the subreflector is at home position, we call the direction cosines of $\hat{N}_j$ with respect to the subreflector frame coordinate axes N^{hp}_{xsj}, N^{hp}_{ysj}, N^{hp}_{zsj} respectively, so that

$$(2.4.2)\quad \hat{N}_j = N^{hp}_{xsj} \cdot \hat{X}_s + N^{hp}_{ysj} \cdot \hat{Y}_s + N^{hp}_{zsj} \cdot \hat{Z}_s \ .$$

These direction cosines are,

$$(2.4.3)\quad \begin{aligned} N^{hp}_{xsj} &= N_{xce} \cdot S_{sce} - N_{yce} \cdot C_{sce} \ , \\ N^{hp}_{ysj} &= N_{xce} \cdot C_{sce} + N_{yce} \cdot C_{sce} \ , \\ N^{hp}_{zsj} &= N_{zce} \ . \end{aligned}$$

Their numerical values are given in Table 7.

Table 7: Target Prism Axis Direction Cosines (Subreflector System) When Subreflector Is At Home Position $\mathbf{S}_{hp}(Az_{com}, EL_{com})$.

(j)	Subreflector	N^{hp}_{xsj}	N^{hp}_{ysj}	N^{hp}_{zsj}
	Target			
ZSG305	Uppermost	-0.5231177	-0.8520017	-0.0209983
ZSG312	Upper Left	-0.0511222	-0.8140772	0.5785021
ZSG313	Upper Right	-0.0503911	-0.8141000	-0.5785342
ZSG316	Lower Left	0.5209365	-0.659346	0.5421142
ZSG317	Lower Right	0.5203756	-0.6591874	-0.5428454
ZSG321	Lowermost	0.8141175	-0.5805874	-0.0114397

When the subreflector is moved to the position specified by the state vector $\mathbf{S}$ the prism axis unit vector is rotated from $\hat{N}_j$ to $\mathcal{R}\left[\hat{N}_j\right] = \hat{N}_j(\mathbf{S})$. The rotated axis vector is computed from the relation:

$$(2.4.4)\quad \mathcal{R}\left[\hat{N}_j\right] = \hat{N}_j(\mathbf{S}) \;=\; N^{hp}_{xsj}\cdot\mathcal{R}\left[\hat{X}_s\right] + N^{hp}_{ysj}\cdot\mathcal{R}\left[\hat{Y}_s\right] + N^{hp}_{zsj}\cdot\mathcal{R}\left[\hat{Z}_s\right] .$$

We now express the rotated axis vector with respect to the subreflector frame basis vectors. We write,

$$(2.4.5)\qquad \hat{N}_j(\mathbf{S}) = \; N_{xsj}(\mathbf{S})\cdot\hat{X}_s + N_{ysj}(\mathbf{S})\cdot\hat{Y}_s + N_{zsj}(\mathbf{S})\cdot\hat{Z}_s \; .$$

The rotated basis vectors have already been computed and are given in (2.3.21). The direction cosines of the prism axis unit vector for general position of the subreflector are then

(2.4.6)

$$N_{xsj}(\mathbf{S}) = N^{hp}_{xsj}\cdot D_{11} + N^{hp}_{ysj}\cdot D_{21} + N^{hp}_{zsj}\cdot D_{31} \; ,$$

$$N_{ysj}(\mathbf{S}) = N^{hp}_{xsj}\cdot D_{12} + N^{hp}_{ysj}\cdot D_{22} + N^{hp}_{zsj}\cdot D_{32} \; ,$$

$$N_{zsj}(\mathbf{S}) = N^{hp}_{xsj}\cdot D_{13} + N^{hp}_{ysj}\cdot D_{23} + N^{hp}_{zsj}\cdot D_{33} \; .$$

The axis direction vector components can now be transformed to either the ground coordinate system or the main reflector coordinate system by available coordinate transforms.

1.6. Summary

In this memo we introduced the concept of a subreflector state vector. This is a convenient device to describe positioning of the subreflector during the complicated motions it undergoes during astronomical observing. By using the device and its associated terminology we can reduce the confusion which has appeared previously when one has discussed motion of the subreflector. It is a natural way to describe subreflector motions. It separates problems associated with driving the subreflector using the telescope control system from problems intrinsic to measurement of subreflector location by laser ranging.

The subreflector positions to which are to be set by the GBT control system will be specified by a sequence of focus tracking messages. Each message provides a state vector which prescribes the subreflector's commanded position and orientation at a particular observing time (and possibly also first and second time derivatives). The state vector components give sufficient information to spatially locate the subreflector's laser target reference points and target prism axis directions. The target reference points are aiming points for the laser rangefinders. When given target reference point positions and axis directions, the metrology system computers can determine target visibility and rangefinder encoder settings for range measurements.

Aiming to subreflector targets (when they are visible) from ground based rangefinders, will not require Finite Element Model calculations. The state vector prescribing the subreflector location provides positional information referenced to the geometric design telescope (corresponding to commanded telescope azimuth and elevation). Ground based rangefinders sit at fixed known locations. Aiming of ground based rangefinders can thus be accomplished without using the telescope's Finite Element Model.

In contrast, feed arm rangefinders are mounted on moving platforms attached to a deformable structure. Their positions and orientations have to be computed using a Finite Element Model, in order to make any ranging measurements. This is a general problem intrinsic to the process of aiming feed arm rangefinders, for all types of range target. That is, feed arm rangefinders require a determination of their positions and orientations, needing finite element analysis, independent of whether they range to the main reflector surface, its rim, the ground, or to the

subreflector. Determination of feed arm rangefinder location has to be accomplished using FEM for all types of rangings from the feed arm, and is not specific to range measurements to the subreflector.

In this document, we have accomplished the following tasks:

We have computed and tabulated fiducial reference point coordinates and prism axis direction cosines for the subreflector prism retrotargets and their associated subreflector surface points, in the subreflector and ellipsoid coordinate systems (Tables 2, 3, 4).

We have computed the distances between pairs of subreflector target reference points and between these reference points and the subreflector optical axis reference point I (Table 2b). These distances are for the temperature at which the subreflector photogrammetry was taken. Aside from a simple temperature correction for thermal expansion, these are constants characteristic to the subreflector and do not change as subreflector position changes. They can be used as entry data for adjustment of ranging measurements to the subreflector.

We have provided equations to calculate subreflector target aim points when given a subreflector state vector request presented by a telescope focus tracking message. We have also provide information needed for computation of target visibility, by supplying the target prism axis direction cosines when the subreflector is in any general position specified by a commanded state vector.

Finally we have provided a scheme to calculate the subreflector translation displacement and rotation from home position, as it sits in place, using as data measured ground or main reflector system coordinates of triples of subreflector target reference points. We have provided a scheme to calculate the rotation of the subreflector frame basis vectors when carried rigidly by the subreflector during a movement from home position; from the rotations of these vectors the subreflector tilt angles may be found corresponding to the subreflector's actual position in space. Numerical parameters needed for these calculations have been provided (Tables 5,6).

This memo is a first analysis to provide detailed subreflector target reference point data and to demonstrate how to use this data to aim rangefinders towards

the subreflector and, inversely, to employ adjusted range-measured subreflector target-reference-point coordinates to specify the subreflector's actual position and orientation in space, which is a first step to obtaining state-vector-parameter data which is needed as error signal information for position feedback control. It is expected that a subsequent study will pursue this program further, and extend and simplify the calculations.

References

Brandt-1

J.J. Brandt. A Protocol For Pointing Synchronization Messages.
GBT Memo 197. NRAO. April 30, 1999.

Goldman-1

GBT Coordinates And Coordinate Transformations.
GBT Memo 165. NRAO. February 15, 1997.

Goldman-2

M.A. Goldman. GBT Laser Ranging System -
Laser Metrology Interface Configuration Diagram.
GBT Drawing D35420K014. May 05, 1997.

Taggart-1

R. Taggart. GBT Archives Drawing D35420M200.
GBT Metrology System - Subreflector Corner Cube Prism Mount.
March 26, 1999.

Wells-1

D. Wells. GBT Subreflector Actuator Functions in C.
GBT Memo 175. NRAO. January 21, 1998.

Wells-2

D. Wells. GBT Gregorian Focus Tracking in C.
GBT Memo 183. NRAO. June 19, 1998.

The Reference Optical Telescope.

The reference optical telescope is just an optical design for a gregorian reflecting telescope with offset optics. Its first optical element is an off-axis surface patch on a paraboloid of revolution. This reflecting patch is designated as the "main reflecting surface" of the telescope. A near-parallel source beam of radiation is focused by this surface patch onto the focus point of the paraboloid, which is designated as the prime focus point of the telescope. The second optical element is an off-axis surface patch on an ellipsoid of revolution. This ellipsoidal patch is designated as the "subreflector surface" of the telescope. The physical structures embodying these surface elements are called the main reflector and secondary reflector of the telescope. (Fig. 1).

One of the two foci of the ellipsoid of revolution is located at the prime focus point, F_0. Radiation leaving the prime focus is reflected by the subreflector surface to the other ellipsoid focus, F_1, the gregorian focus of the telescope (also called the M1 focus). The line through the two foci is the major axis of the ellipsoid.

The paraboloid and ellipsoid axes intersect at the prime focus point, which is a common focus of those two quadric surfaces. These axes intersect at an angle β ($0 < \beta << 90°$). The plane passing though them defines the "tangential optical plane". Each surface patch is defined furthermore to be generated by the intersection of a plane perpendicular to the tangential plane with its defining quadric; such a plane cuts off a surface patch which is symmetric with respect to the tangential optical plane. The tangential optical plane is then a plane of symmetry of each reflecting surface and bisects it, and is also a unique plane of symmetry of the telescope. Let I_1 be the point in the tangential optical plane which defines the mid ray of the tangential fan of rays from the gregorian focus to the subreflector surface.

The gregorian focal plane of the optical telescope passes through the focus F_1

and is perpendicular to the ray I_1F_1. The rays I_1F_1 and F_0I_1 can be considered to define a (folded) optical axis of the telescope.

In a physical embodiment of the telescope the gregorian focal plane will coincide with flat machined surfaces of flanges attached to the receiver room turret's platter structure. The platter axis will be aligned perpendicular to the flanges and the focal plane. The flanges mate to flanges on the individual receiver support mounts. The platter flange centers, ideally, lie on a 56 inch radius circle centered on the turret axis, offset 56 inches from the gregorian focus. The receivers are rotated as required to the gregorian focus.

The turret platter is provided with eight receptacles on its perimeter, one for each receiver assembly. Each receptacle has three feed positioning slots (for the cardinal feed position, and three degrees on either side of the cardinal position). An index pin and motorized actuator is mounted on the ceiling of the feed room diametrically opposite the active feed. The receiver feed is locked into position by driving the index pin radially inward towards the turret axis, and engaging a slot on the appropriate receptacle.

The telescope's optical design is defined by the following parameters:

1. The focal length, f_p, of the paraboloid.
2. The angle, β , between the ellipsoid and paraboloid axes.
3. The eccentricity, e , of the ellipsoid.
4. The spacing, $2f_e$, between foci of the ellipsoid.
5. The offset angle, α, from the ellipsoid major axis, of the mid ray of the tangential plane ray fan from the gregorian focus to the subreflector.
6. The half-angle, Θ_H , of the tangential plane ray fan from the gregorian focus to the subreflector surface.
7. The half-angle, Θ^* , of the tangential plane ray fan from the prime focus to the intersection of the main reflector surface with the tangential plane.
8. The offset angle, Θ_0 , from the paraboloid axis, of the mid ray of the tangential plane ray fan from the prime focus to the parabolic arc intersection of the main reflector surface.

The reference optical design has been specified by Norrod and Srikanth in GBT Memo 155 [Nor-1]. The exact parameters of the optical telescope specified in this memo are:

f_p	6000 cm
β	5.570°
e	0.528
$2f_e$	1100 cm
α	17.899°
Θ_H	14.99°
Θ^*	42.825°
Θ_0	39.005° .

When referring to the optical telescope we use the following notation. Let:

V_0 denote the paraboloid vertex.

F_0 denote the prime focus point, the common focus of the ellipsoid and paraboloid.

F_1 denote the gregorian focus point, which is the other focus of the ellipsoid.

I_1 denote the intersection point of the tangential plane mid ray from the gregorian focus, with the subreflector surface.

a be the length of the major semi axis of the ellipsoid.

b be the length of the minor semi axis of the ellipsoid.

r_1 be the length of the ray F_1I_1 .

r_2 be the length of the ray F_0I_1 .

d_{sp} be the perpendicular distance of point I_1 to the paraboloid axis.

h_{sp} be the projected length of ray F_0I_1 along the paraboloid axis.

d_{mp} be the perpendicular distance of point F_1 to the paraboloid axis.

h_{mp} be the projected length of ray F_0F_1 along the paraboloid axis.

γ be the angle $F_0I_1F_1$.

The following geometric relations hold:

(2.1) $\quad a = \dfrac{f_e}{e}$,

(2.2) $\quad b = a\sqrt{1-e^2}$,

(2.3) $\quad r_1 + r_2 = 2a$.

Applying the law of cosines to triangle $F_0F_1I_1$ and using (2.3) one gets

(2.4) $\quad r_1 = \dfrac{f_e\,(\dfrac{1}{e} - e)}{1 - e\cos\alpha}$, $\quad r_2 = 2a - r_1$.

Applying the law of sines to the same triangle one gets

(2.5) $\quad \gamma = \sin^{-1}\left[(\dfrac{2f_e}{r_2})\,(\sin\alpha)\right]$.

By simple trigonometry,

(2.6) $\quad d_{sp} = r_2\ \sin(\alpha + \gamma - \beta)$, $\quad h_{sp} = r_2\ \cos(\alpha + \gamma - \beta)$.

(2.7) $\quad d_{mp} = 2\,f_e\,\sin(\beta)$, $\quad h_{mp} = 2\,f_e\,\cos(\beta)$.

The unit outward normal vector to the ellipsoidal surface patch at I_1 makes an angle $(\dfrac{\gamma}{2}) + \alpha$ with the ellipsoid's major axis and makes an angle $(\dfrac{\gamma}{2}) + \alpha - \beta$ with the paraboloid's axis.

The derived parameters of the reference optical design are:

Derived Parameter	Stated Value In GBT Document	Computed From (2.1)-(2.7)
a	410.106" (*)	1041.6667 cm (410.1050")
b	348.280" (*)	884.6296 cm (348.2794")
r_1	1510 cm (†)	1509.9158 cm (594.4550")
r_2	573 cm (†)	573.41748 cm (225.7549")
γ		36.127028°
d_{sp}	429.200 cm (‡)	429.1726 cm (168.9656")
h_{sp}	380.300 cm (‡)	380.2874 cm (149.7194")
$(\frac{\gamma}{2}) + \alpha$		35.962514°
$(\frac{\gamma}{2}) + \alpha - \beta$		30.392514°
d_{mp}	106.800 cm (‡)	106.7680 cm (42.0346")
h_{mp}	1094.800 cm (‡)	1094.8062 cm (431.0261")

The optical geometry of the subreflector is illustrated in Fig. 1.

* RSI Contractor's Drawing 120730 .
† GBT Memo 155
‡ GBT Drawing C35102M081-Rev. B-Sheet 1. Design values on this drawing are optical design values, rounded to the nearest millimeter.

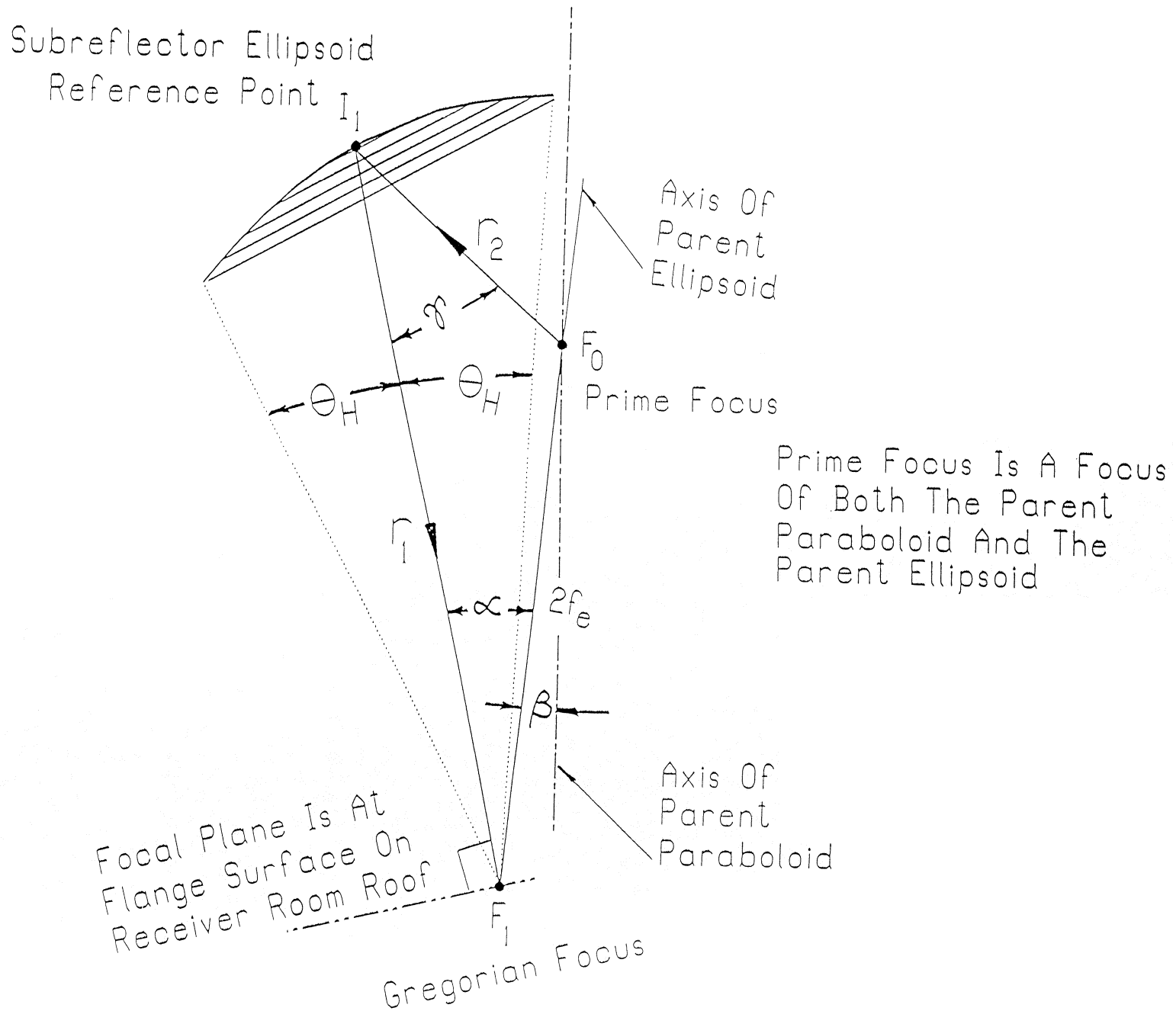

Figure 1. The Subreflector Ellipsoid Reference Geometry

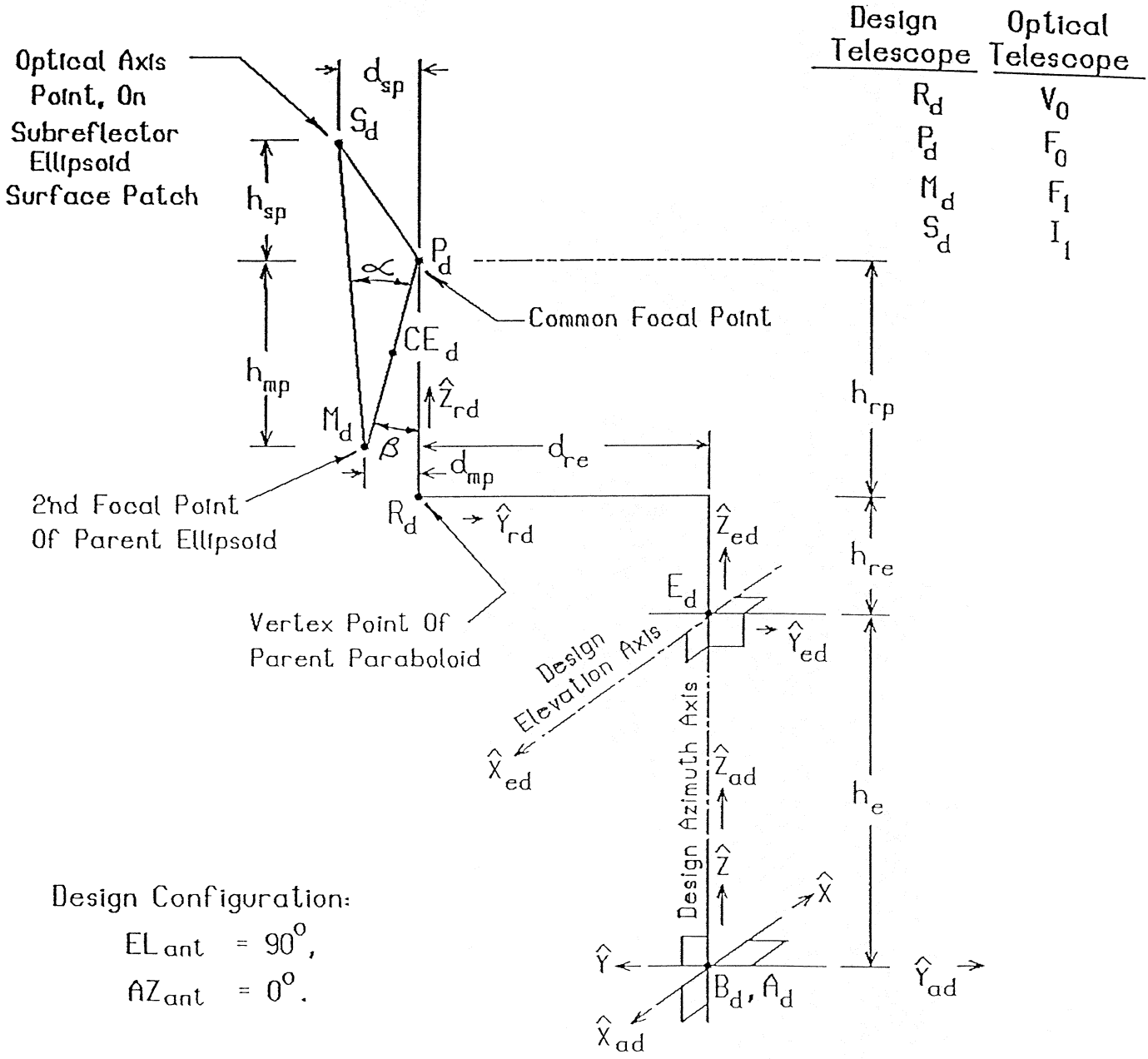

Design Configuration:

$EL_{ant} = 90^o$,

$AZ_{ant} = 0^o$.

Figure 2. Design Telescope Reference Points

GBT Prime Focus Receiver Mount
Adjustment Specifications

NOTES:
1. Xp AND Yp LIE IN ANTENNA PLANE OF SYMMETRY.
2. REF: RSI DWG 121039

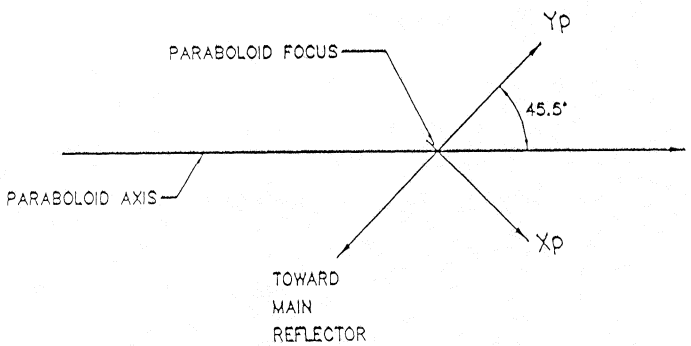

GBT Subreflector Mount
Adjustment Specifications

NOTES:
1. Xs AND Ys LIE IN ANTENNA PLANE OF SYMMETRY.
2. Zs IS PERPENDICULAR TO Xs AND Ys.
3. REF: RSI DWG 121038

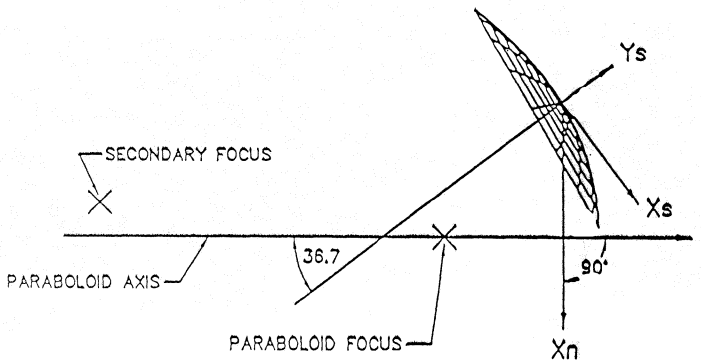

Figure 3.

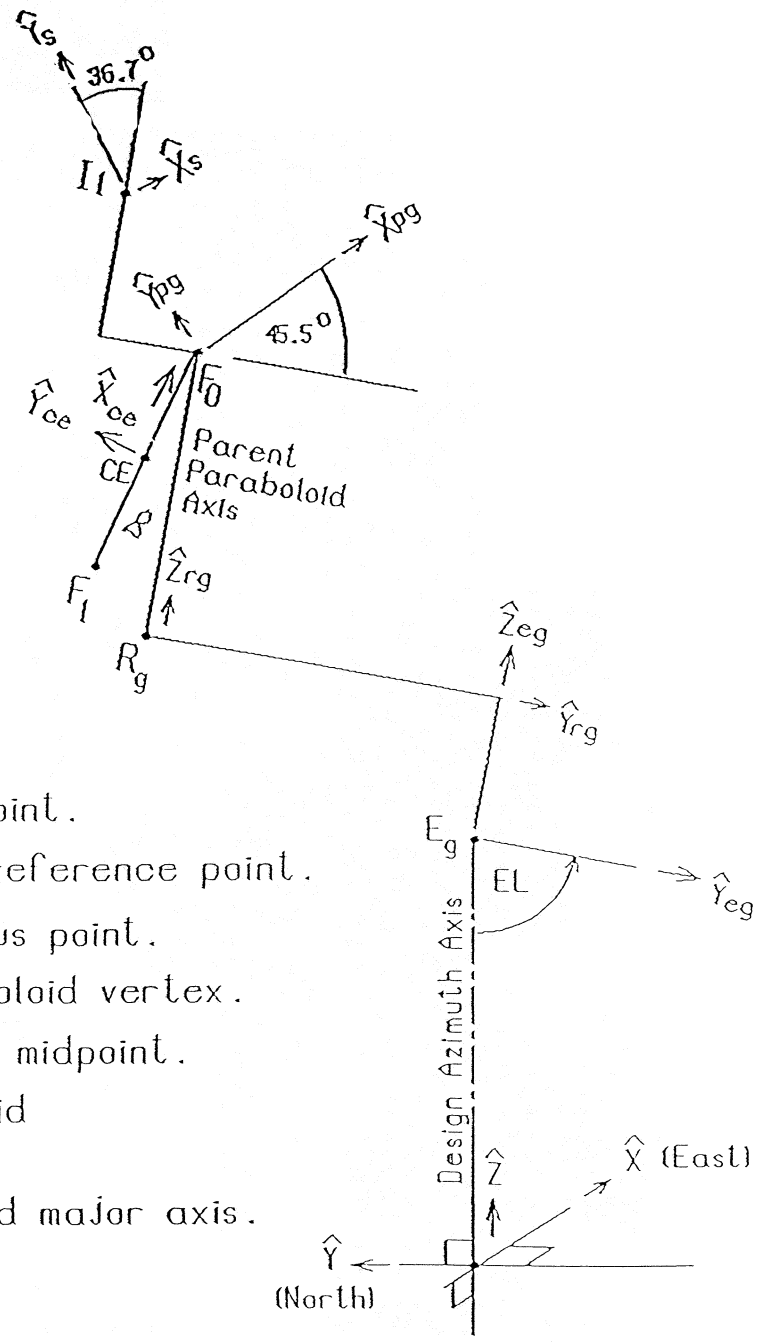

EL is the antenna elevation angle.

F_0 is the prime focus point.

I_1 is the subreflector reference point.

F_1 is the gregorian focus point.

R_g is the parent paraboloid vertex.

E_g is the elevation axle midpoint.

CE is the parent ellipsoid center point.

$\hat{X}_{ce}$ is along the ellipsoid major axis.

Figure 4. Geometric Telescope Unit Base Vectors.

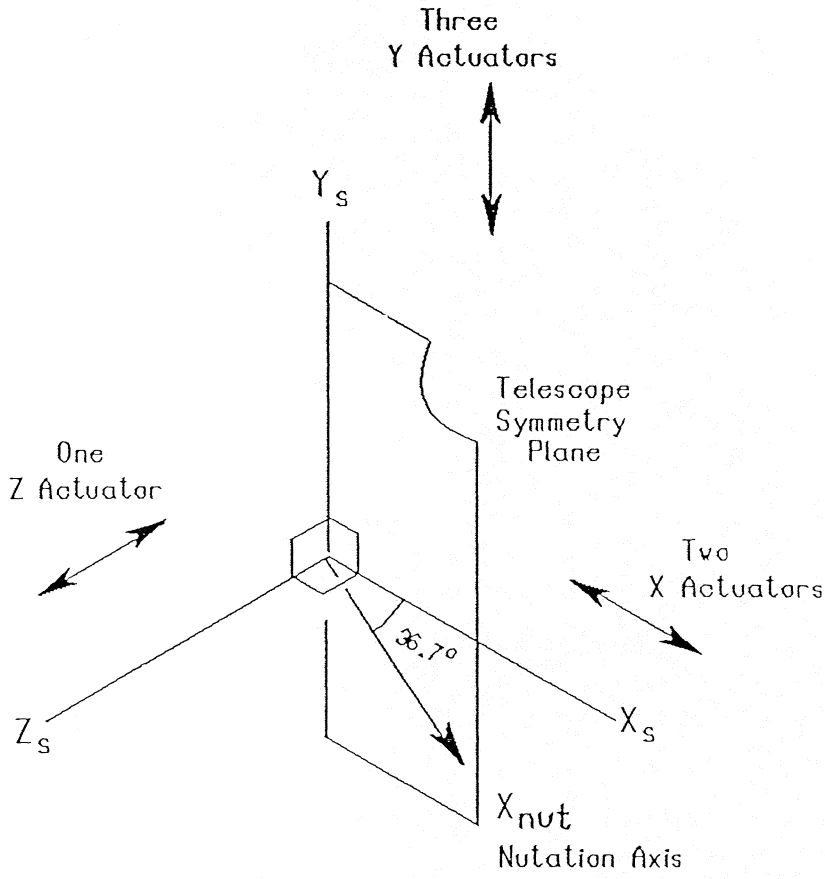

Figure 5. Reference Directions For Subreflector Motions.

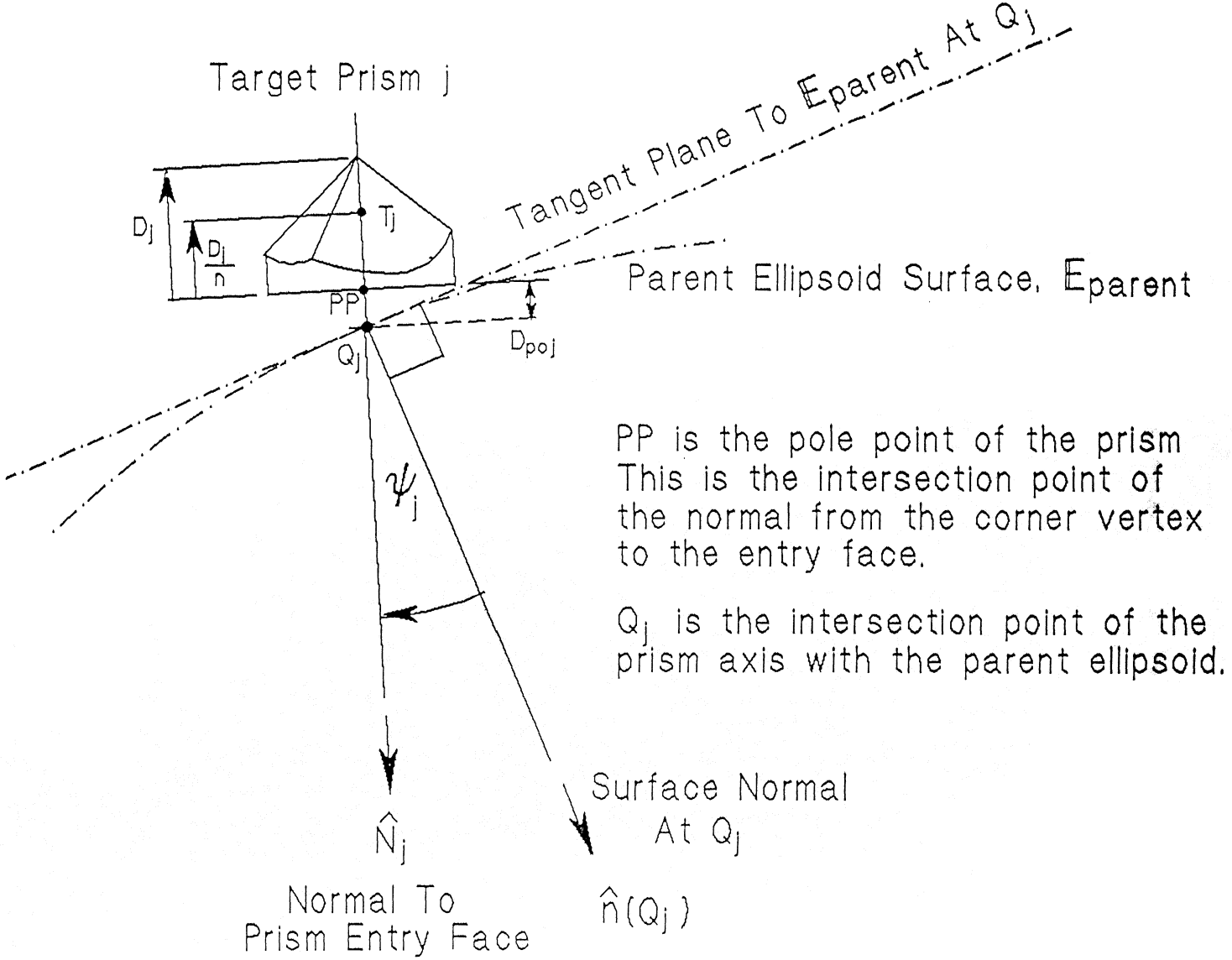

Figure 6. Subreflector Prism Geometry

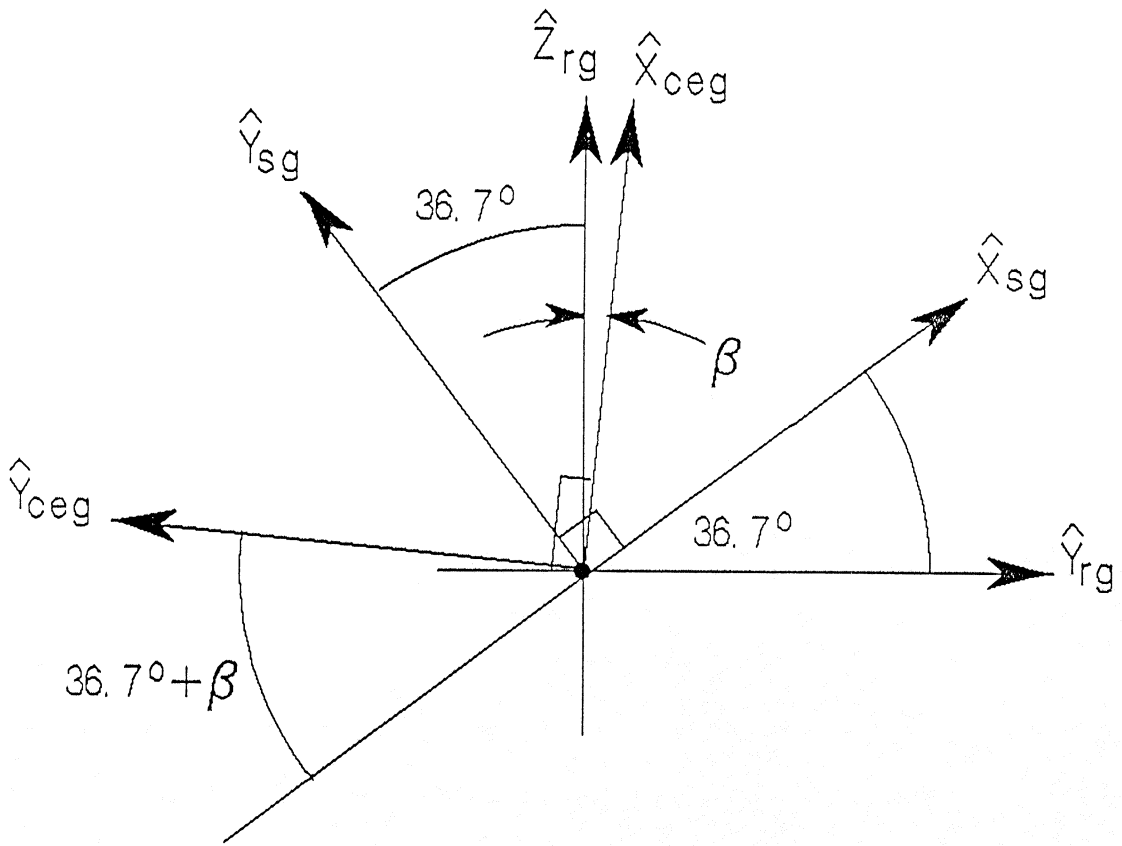

Figure 7. Relative Basis Vector Directions.

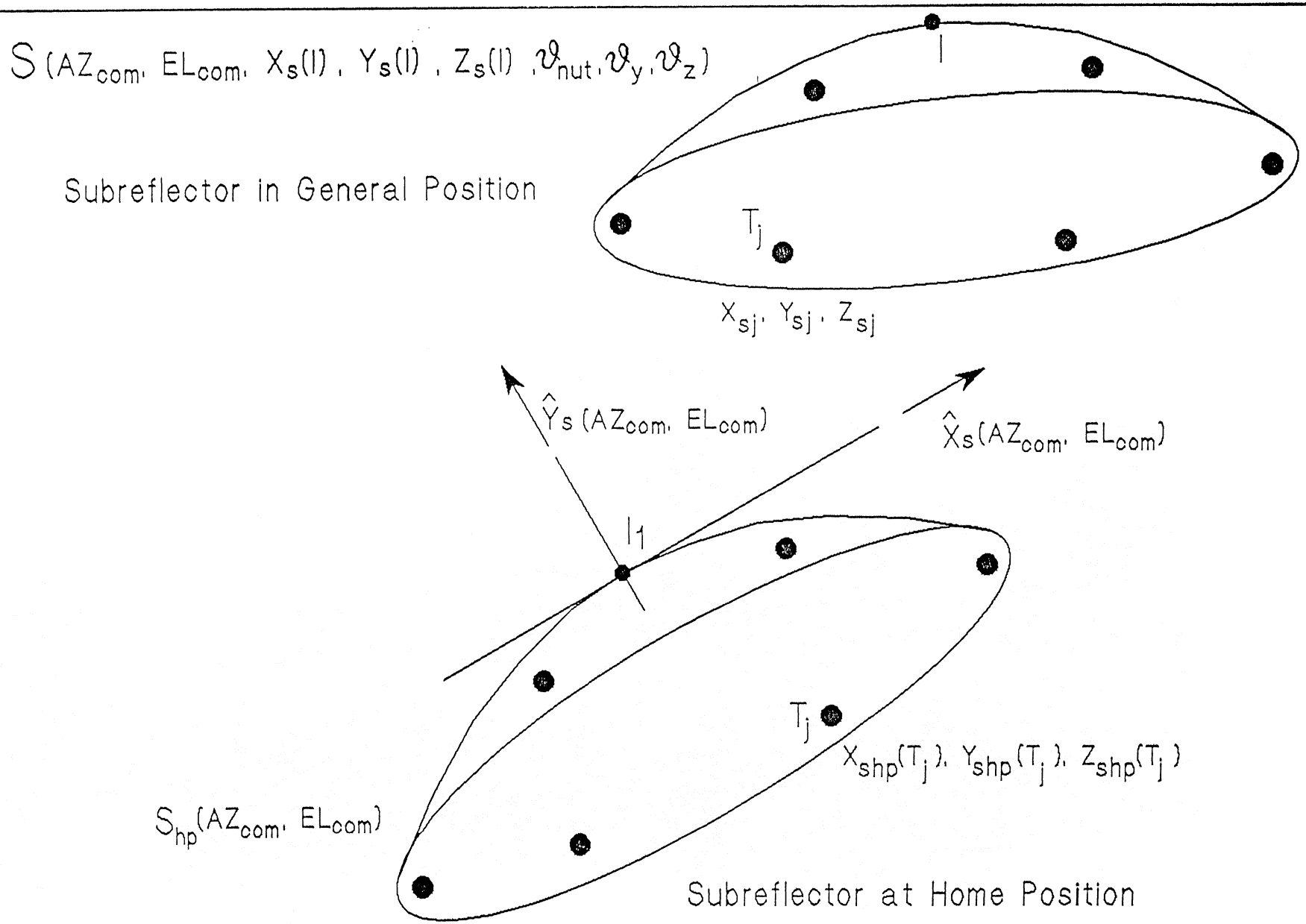

Figure 8. State Vector Specification Of Subreflector Target Location.

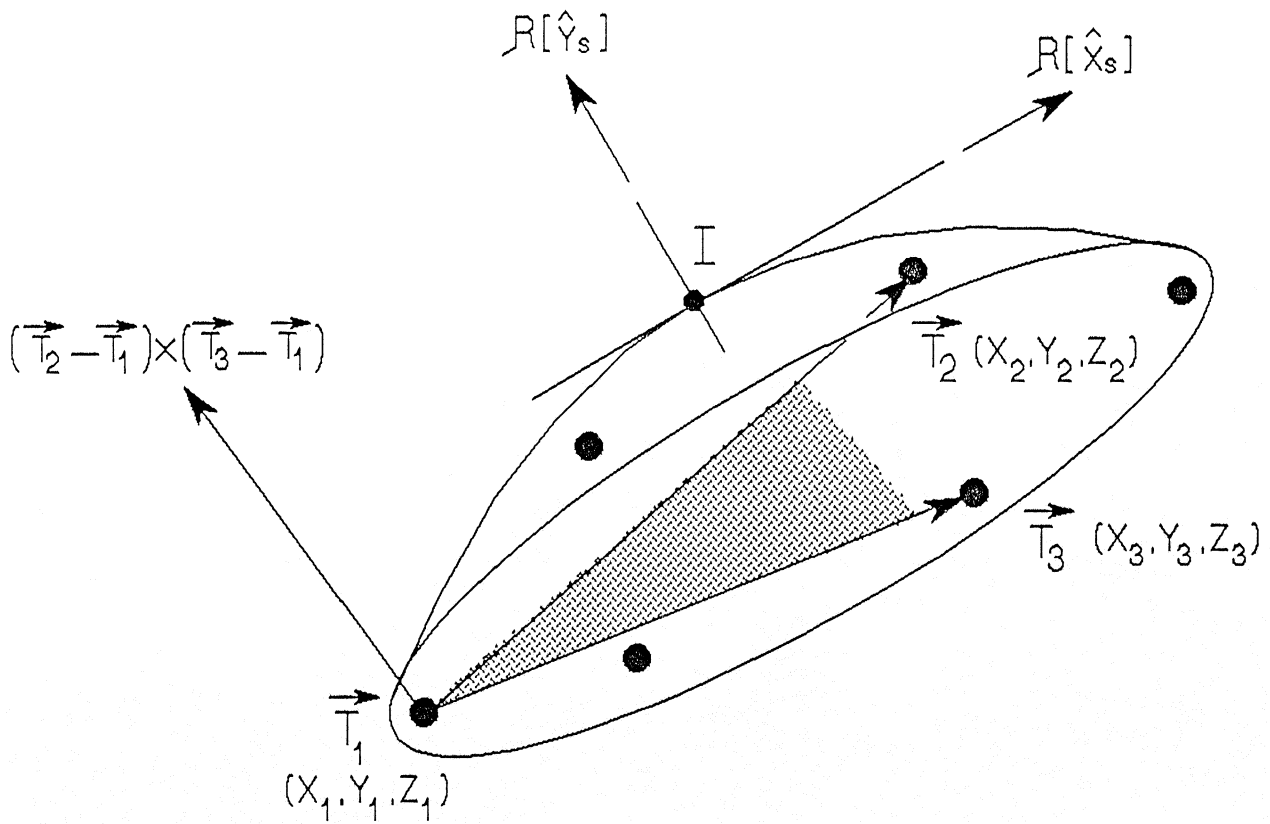

Figure 9. Determination Of Subreflector Location From Target Coordinates.

REVISIONS					
REVISION	MADE BY	DESCRIPTION	ZONE	DATE	APPROVED
A	R. TACCART	AS BUILT DESIGN CHANGES	ALL	07/08/99	

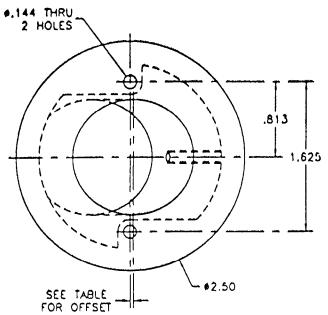

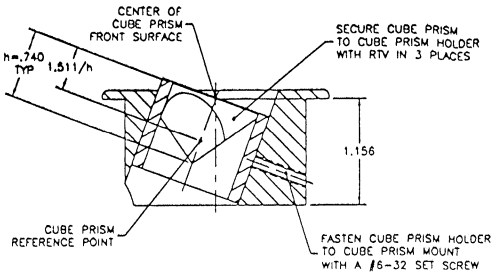

SECTIONAL ASSEMBLY

SCALE: 1.5X

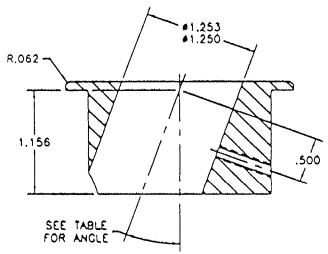

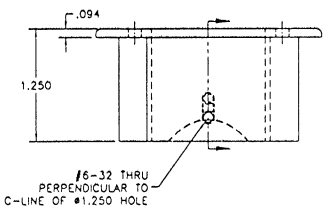

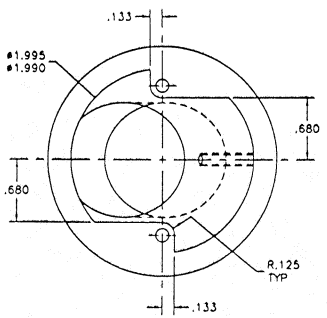

MOUNT #	ANGLE	OFFSET	# REQUIRED
1	3.8°	.006	1
2	20.1°	.034	2
3	32.1°	.059	2
4	37.2°	.071	1

CUBE PRISM MOUNT

SCALE: 1.5X
MATERIAL: ALUMINUM
FINISH: CHROMATE & GOLDSTONE 500 PAINT

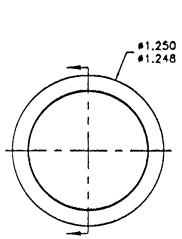

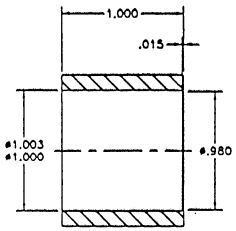

CUBE PRISM HOLDER

SCALE: 2X
MATERIAL: ALUMINUM
FINISH: CHROMATE & GOLDSTONE 500 PAINT
6 REQUIRED

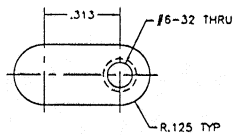

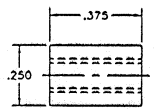

FASTENING TAB

SCALE: 4X
MATERIAL: ALUMINUM
FINISH: CHROMATE & GOLDSTONE 500 PAINT
2 REQUIRED PER MOUNT

NATIONAL RADIO ASTRONOMY OBSERVATORY			
PROJECT/TITLE: CBT METROLOGY SYSTEM SUBREFLECTOR CORNER CUBE PRISM MOUNT			
DRAWN: R. TACCART	CHECKED: R. TACCART	DATE: 03/26/99	
SCALE: AS NOTED	GENERAL: AS NOTED	FINISH: AS NOTED	
FILE: DRAWINGS\MECHMC\35420\M200	SHEET: 1 OF 1	REVISION: A	DRAWING NO. 035420M200